arXiv:2007.05637v3 [cs.DS] 4 Dec 2020

Dynamic Graph Streaming Algorithm for Digital Contact Tracing

Gautam Mahapatra, Priodyuti Pradhan, Ranjan Chattaraj and Soumya Banerjee

Abstract—Digital contact tracing of an infected person, testing the possible infection for the contacted persons, and isolation play a crucial role in alleviating the outbreak. Here, we design a dynamic graph streaming algorithm that can trace the contacts under the control of the Public Health Authorities (PHA). Our algorithm receives proximity data from the mobile devices as contact data streams and uses a sliding window model to construct a dynamic contact graph sketch. Prominently, we introduce the edge label of the contact graph as a binary contact vector, which acts like a sliding window and holds the latest D days (incubation period) of temporal social interactions. Notably, the algorithm prepares the direct and indirect (multilevel) contact list from the contact graph sketch for a given set of infected persons. Finally, the algorithm also uses a disjoint set data structure to construct the infection pathways for the trace list. The present study offers the design of algorithms with underlying data structures for digital contact trace relevant to the proximity data produced by Bluetooth enabled mobile devices. Our analysis reveals that for COVID-19 close contact parameters, the storage space requires maintaining the contact graph of ten million users; having 14 days of close contact data in the PHA server takes 55 Gigabytes of memory and preparation of the contact list for a given set of the infected person depends on the size of the infected list. Our centralized digital contact tracing framework can also be applicable for other relevant diseases parameterized by an incubation period and proximity duration of contacts.

Index Terms—Contact graph, streaming algorithm, sliding window model, Bluetooth, disjoint set, COVID-19.

1 Introduction

Delaying in the vaccine or drug design increases the rapid spread of the COVID-19 disease. The current COVID-19 pandemic is caused by the droplet-based human to human transmission of SARS-CoV-2 [1]. At present, the whole human society is anxiously waiting for a possible new normal state of living. Almost every country adopted the social distancing and lockdown to mitigate the pandemic [2]. Although complete lockdown reduced the risk of spread, extending the lockdown created severe problems for the economy and the social life of the countries [3]. Also, as the pandemic stays a long time in a country, it becomes challenging to maintain the lockdown. Many countries eased the lockdown in terms of alternating and intermittent lockdown strategies to balance between infection spread and economy [3], [4]. In this scenario, currently developed smartphone-based digital contact tracing becomes a promising approach to control the pandemic [1], [5], [6]. A recent study shows that highly effective contact tracing and case isolation are good strategies to control a new outbreak of COVID-19 [7]. Another study suggests to get normality, which takes at least a couple of years, and at the same time, we should prepare for the next pandemic [8].

Contact tracing was a common and successful step to control several infectious diseases (e.g., Zika, HIV, influenza, Ebola viruses) [9], [10]. The World Health Organisation (WHO) defines contact tracing as the identification and follow-up of persons who may contact an infected person [9]. For COVID-19, two persons are in close contact if they are exposed to each other for at least fifteen minutes within one meter of distance [9]. The goal of contact tracing is to reduce a disease's effective reproductive number (R_0) by identifying people who have been exposed to the virus through the said close contact with an infected person and listing them for immediate quarantine or isolation. It has been reported that 46% contribution to R_0 comes from the presymptomatic individual (before showing symptoms) for COVID-19 [11]. On the other hand, COVID-19 infection is mostly asymptomatic in nature. Hence, highly effective direct and indirect contact tracing is a mandatory task and plays a crucial role in early

- *Gautam Mahapatra is associated with Department of Computer Science, Asutosh College, University of Calcutta, Kolkata, West Bengal, India and Department of Computer Science and Engineering, Birla Institute of Technology, Mesra, Off-Campus Deoghar, Jharkhand, India. E-mail: gsp2ster@gmail.com*
- *Priodyuti Pradhan is associated with Complex Network Dynamics Lab, Department of Mathematics, Bar-Ilan University, Ramat-Gan, Israel. E-mail: priodyutipradhan@gmail.com*
- *Ranjan Chattaraj is associated with Department of Mathematics, Birla Institute of Technology, Mesra, Off-Campus Deoghar, Jharkhand, India. E-mail: chattaraj6@gmail.com*
- *Soumya Banerjee is associated with Inria EVA, Paris, France & Director Innovation Smart City EU. E-mail: dr.soumyabanerjee@ieee.org*

infection detection and reduces the peak burden on the healthcare system. Due to higher uncertainties in social relations, manual contact tracing to find the contact structure is very complicated for the PHA [12]. Recently, digital contact tracing uses low power radio frequency-based Bluetooth enabled mobile devices to overcome the problems in manual contact tracing. The success of TraceTogether of Singapore Government [13], COVID-Watch of Stanford University [14], [15], PACT of MIT [16], Exposure Notification forthcoming App of Apple-Google [17], Arogya Setu of MoHFA, Government of India [18] are all recent developments based on the Bluetooth technology to prepare the contact list more effectively to mitigate the COVID-19 pandemic [11], [19], [20], [21], [22], [23].

Although digital contact tracing substantially reduces human efforts of manual contact tracing, most smartphone apps store data locally in the device memory to maintain privacy [10]. Hence, the central authority has no control over the contact data. After detecting an infected person, PHA requests the person to donate the app data to make the trace list. As we know, a country's public health infrastructure is a national asset for which the government is responsible, and no pandemic can be addressed without a functional health system of the country [24]. On the other hand, the existing app provides only the direct contact tracing facility, but indirect contact tracing also plays a vital role in mitigating the spread and reducing the death rate [25]. Hence, to automate the trace list preparation in a regular interval, all proximity data should be automatically fetched by the PHA server from the registered devices and immediately store in the form of ready to process structure. However, in the pandemic period, the vital question is how does the centralized control system store a large number of device data as well as prepare direct and indirect contact lists about which little is known and remains elusive [26].

This article provides a one-pass dynamic graph streaming algorithm with a sophisticated data structure to automate the multi-level digital contact tracing more accurately and efficiently by having centralized control under the PHA. After receiving the proximity data stream from the mobile devices, the algorithm uses a sliding window model to process the proximity data and dynamically evolves a close contact graph sketch (Fig. 1). The nodes in the close contact graph are the individual users, and an edge is included if there exists an interaction between a pair of people for more than τ minutes (proximity duration) in D days (incubation period) [27]. Importantly, we introduce an edge label (interactions) between a pair of the individual in the contact graph as a fixed-sized binary first-in-first-out (FIFO) contact vector to store the temporal information in the last D days, and earlier data are automatically leaving from the system storage. In other words, during a pandemic, the contact graph stores the latest D days of continuous close contact data in a discrete form inside contact vectors. Finally, the system prepares the contact list for the given infected persons from the contact graph. We wish to emphasize that our algorithm prepares the direct and indirect (multi-level) contact list of the infected persons and stores it in disjoint sets to find the infection pathways. We use the index file structure to store the large contact graph for fast accessing. The system's salient feature is that it automatically removes the inactive edge when the D days over and updates the graph through a sliding window model over the contact vectors. We provide implementation details and analysis of our devised streaming algorithm. Remarkably, our analysis reveals that for COVID-19 contact trace parameters, to store the contact graph for 14 days for 10^7, users take 55 GB of memory space. Besides, the preparation of the contact list for a given set of infected persons depends on the size of the infected list. Our algorithm is simple and easy to implement. By considering the location and time-independent binary contact vectors and making centralized control by the PHA, our algorithm maintains the individuals' privacy. We expect it to be an attractive choice to deploy in the application of digital contact traces in real-world pandemic situations.

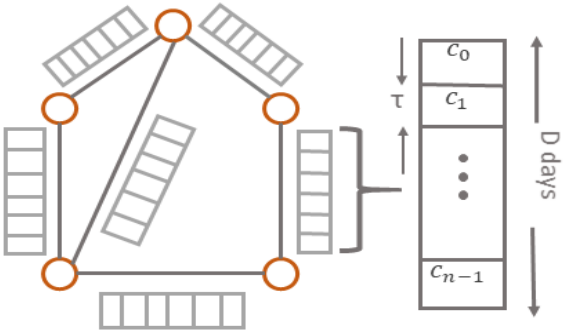


Fig. 1. Schematic representation of close contact graph ($\mathcal{G}$). We introduce edge label of $\mathcal{G}$ as binary vector ($\boldsymbol{c}$). Here, D is the incubation period, τ is the time slot for exposure. For COVID-19, $D = 14$ and $\tau = 15$ minutes. We set c_k to be 1, when a close contact is detected at the k^{th} time slot duration and 0 otherwise.

We fabricate the article as follows: Section 2 discusses the problem formulation and methodology of the digital contact tracing process. Section 3 provides implementation detail of our dynamic graph streaming algorithm with sliding window model. Section 4 contains the space complexity of the contact graph and analyzes the contact trace algorithm. Finally, Section 5 summarizes our work and discusses various open problems for further investigations.

Symbols and Notations	Description
τ, D	Close contact parameters – minimum time duration spend for close contact (proximity duration) and latest observation period in days (incubation period)
$\boldsymbol{c}_{(P,P')}$	Contact vector – between individuals P and $P^{'}$.
σ	Contact trace operator – a binary operator for indirect (multi-level) contact tracing.
$P \rightsquigarrow P^{'}$	flow of infection elements from P to $P^{'}$
$\mathcal{G}$	Close contact graph – having two components (i) ($\mathcal{G}.\Phi$) stores addresses of the close contact vectors (ii) $\mathcal{G}.\Theta$ stores close contact vectors.
$\Sigma, \mathcal{I}, \Gamma$, and χ	population having smartphones, infected persons, suspected individuals or contact trace list, directed edges for infection transmission pathways
δ	sampling time interval for smartphone.
Ω and $\mathcal{W}$	Data stream – received from smartphones to PHA server and sliding window
T and t	System start time and beginning time of the proximity contacts data in Ω.
L	Levels of indirect contact tracing
$\mathcal{F}$	Disjoint set data structure for efficient representation of the infection transmission that are determined by contact trace operation (χ) on the contact graph $\mathcal{G}$.

TABLE 1
List of symbols and notations.

2 Methodology and Results

Infectious diseases caused by microscopic germs such as bacteria or viruses are called the infection elements that get into the human body and cause health problems. Infectious diseases that spread from person to person are said to be contagious. One of the essential non-pharmaceutical methods to mitigate the outbreak of infectious disease is contact tracing [28]. Contact tracing means identifying everyone who comes directly or indirectly with an infected (symptomatic/asymptomatic) person. These contacts are then identified and monitored for D days to see if they start showing symptoms. Suppose a contact begins to show any disease symptoms. In that case, the person is immediately isolated, quarantined, tested, provided care, and the cycle starts again. All of the new infected persons' contacts must be distinguished and monitored for D days for disease symptoms to see if they become infected. The process repeats until there are no new infections found. For instance, incubation period for Ebola $D = 21$, Influenza $D = 5$, and for COVID-19, $D = 14$ [28], [29].

For the digital contact tracing system, a population (Σ), is a set of individuals under a particular Public Health Authority (PHA) who use their smartphones. For human nature of social interactions, any two individuals $P, P^{'} \in \Sigma$, we define P is in *close contact* of $P^{'}$ or $P^{'}$ is in *close contact* of P, if during last D days, P and $P^{'}$ are in proximity of contact within d meters of distance for at least τ minutes [27]. For a particular contagious disease, d (proximity distance), τ (proximity duration), and D (incubation period) are parameters of *close contact*, respectively. Importantly, when P and $P^{'}$ come in close contact, they have no symptoms of the disease but may carry infection elements. Even they do not know each other, i.e.; privacy should be maintained during a close contact. On the other hand, they also meet with each other several times; thus, several close contacts between P and $P^{'}$ in D days. If anyone has the infection, it will show the symptoms within the next D days. Therefore, it is essential to hold the temporal information of the close contact for the next D days to find the contact list for an infected person.

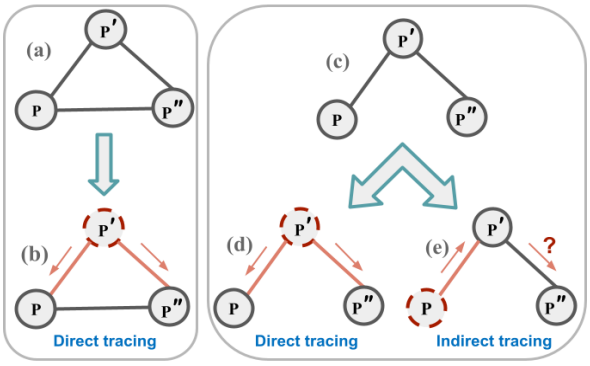


Fig. 2. Illustration of direct and Indirect contact tracing.

To illustrate close contact, we consider three individuals (P, $P^{'}$, and $P^{''}$) and their possible close contacts (Fig. 2 (a-d). One can observe that if $P^{'}$ is detected as an infected person ($\mathcal{I} = \{P^{'}\}$) within D days of the close contact then P and $P^{''}$ belongs to the *close contact trace list* denoted as $\Gamma_{P^{'}} = \{P, P^{''}\}$ of $P^{'}$ (Fig. 2(b) and (d)). Here, $\{P, P^{''}\}$ are represented as *direct* contact of an infected person $P^{'}$. We wish to show another complex situation, which is also very important to trace and help to reduce the spread of the disease [25]. Suppose in Fig. 2 (c) and (e), P is detected as an infected person, then $P^{'}$ should be in the direct contact list of P i.e., $\Gamma_P = \{P^{'}\}$. However, whether $P^{''}$ should be in the contact list of P or not? To decide, we should analyze the temporal

information between $(P, P^{'})$ and $(P^{'}, P^{''})$ and which is challenging due to store all close contacts for the last D days and accurate analysis of ordering. We refer $P^{''}$ as indirect contact for P. Here, $P^{''}$ will be in the trace list Γ_P, if $P^{''}$ has a close contact with $P^{'}$ during or after the close contact between $P^{'}$ and P within D days. To capture the direct and indirect contact tracing, we store the temporal information inside the circular queue working like a serial-in-serial-out shift register to hold all close contacts only for the latest D days, and we refer to it as a *close contact vector*. Importantly, to decide there is any indirect contact or not? we introduce a binary operator refer to as *close contact trace* operator denote as σ which operates on two contact vector between $(P, P^{'})$ and $(P^{'}, P^{''})$ and returns a TRUE/FALSE decision. Hence, formally a contact tracing system for a contagious disease must store all *close contact* information of the whole population Σ for the last D days. Thus, at any time for a given set of infected individuals ($\mathcal{I}$), the system can determine the close contact trace list or suspected persons (Γ). For simplicity, we assume once an individual is detected as a laboratory-confirmed infected person, immediately contact tracing is carried out and infected, as well as all suspected individuals are being isolated so that they are not contacting further.

There are two major components of the contact tracing system: **module 1** (mobile app) – data acquisition by smartphones – continuous capturing of the enormous asynchronous analog social contacts events through Bluetooth enabled devices, subsequently conversion into discrete form and send to the server, **module 2** – computation on PHA server: a) analyze the discrete mobile app data stream to identify close contacts, (b) use the efficient storage representation to hold all such close contact data for the last D days period, (c) design an effective contact tracing algorithm working on such voluminous data to generate contact trace results within a reasonable time, and (d) finally, represent outputs in an efficient form so that it can be used to show infection pathways.

We only focus on the algorithm and implementation of the contact tracing system on the PHA server-side **(module 2)**. Note that in practical situations, all individuals under PHA are not using smartphones and hence not included in Σ. It is predicted that by 2021, there will be 3.8 billion of smartphone users for the world population of 7.8 billion [30]. Therefore, we can bring almost half of the world population under a digital contact tracing system by efficiently implement it. The following section discusses the digitization into close contact vector, close contact graph construction, and contact tracing processing in detail.

2.1 Digitization of Close Contacts

To identify *close contacts* between any pair of individuals P and $P^{'}$, PHA server subdivides the D days into $n = \lceil \frac{24\times 60\times D}{\tau} \rceil$ slots each of τ minutes consecutive intervals and digitized as *close contact vector* ($\boldsymbol{c}_{(P,P')} = (c_{n-1}, \ldots c_1, c_0)$). Here, $c_i^{'}s$ are different consecutive time slots, c_0 is the latest, and c_{n-1} is the earliest (Fig. 1). Importantly, $\boldsymbol{c}_{(P,P')}$ is a FIFO vector because it has fixed n numbers of binary components, and as time advances to the first slot of $(D+1)^{th}$ day, then the earliest slot at c_{n-1} exit to accommodate a new input slot at c_0 (Fig. 1). We associate one bit for each slot in the digital form of the *close contact* vector. By default all n bits are ZERO, and a bit is set to ONE, if P and $P^{'}$ come close to each other in the past D days. It can also happen that several times or for consecutive times, both are close to each other; thus, several bits in $\boldsymbol{c}_{(P,P')}$ are set to ONE. In brief, our system converts continuous sensor data into discrete close contact slots, and store in a binary form in PHA server. For instance, To identify every close contact in the COVID-19 pandemic, we subdivide the $D = 14$ days into $\tau = 15$ minutes time slots (i.e., n slots) and store one bit if there is a proximity contact in a particular time slot.

Additionally, to maintain the privacy of the close contact information between two individuals PHA server distributes virtual IDs to the smartphone devices for proximity communications. All the sampled discretized proximity-based contact data appear to the PHA server in the form of a data stream and analyzed by the PHA server to extract the actual user ID to identify the close contacts. Finally, the PHA server constructs the contact vectors and stores them in the close contact graph. In the following section, we discuss contact vectors as temporal information on the dynamic close contact graph sketch.

2.2 Contact Graph

To store all *close contact* information for last D days among all the individuals, we introduce close contact graph $\mathcal{G} = (V, E)$. Here, vertices of $\mathcal{G}$ are the smartphone-enabled individuals i.e. $V = \Sigma$, and if, in last D days there is any *close contact* between two individuals, i.e., vertices $P, P^{'} \in \Sigma$ then we have an edge, $e_i = (P, P^{'}, \boldsymbol{c}_{(P,P')})$ between them, and store the temporal close contact information as bits inside contact vector $\boldsymbol{c}_{(P,P')}$. Note that whenever we include/update the edge relation and the associated contact vector, the system does not know whether the individual is infected or not. Hence, the edges of the contact graph are always undirected ($\boldsymbol{c}_{(P,P')} = \boldsymbol{c}_{(P',P)}$). More importantly, *$\mathcal{G}$ only stores the close contact information for D days as undirected edges with Contact vector as edge label*. The $\mathcal{G}$ is not holding any information about the

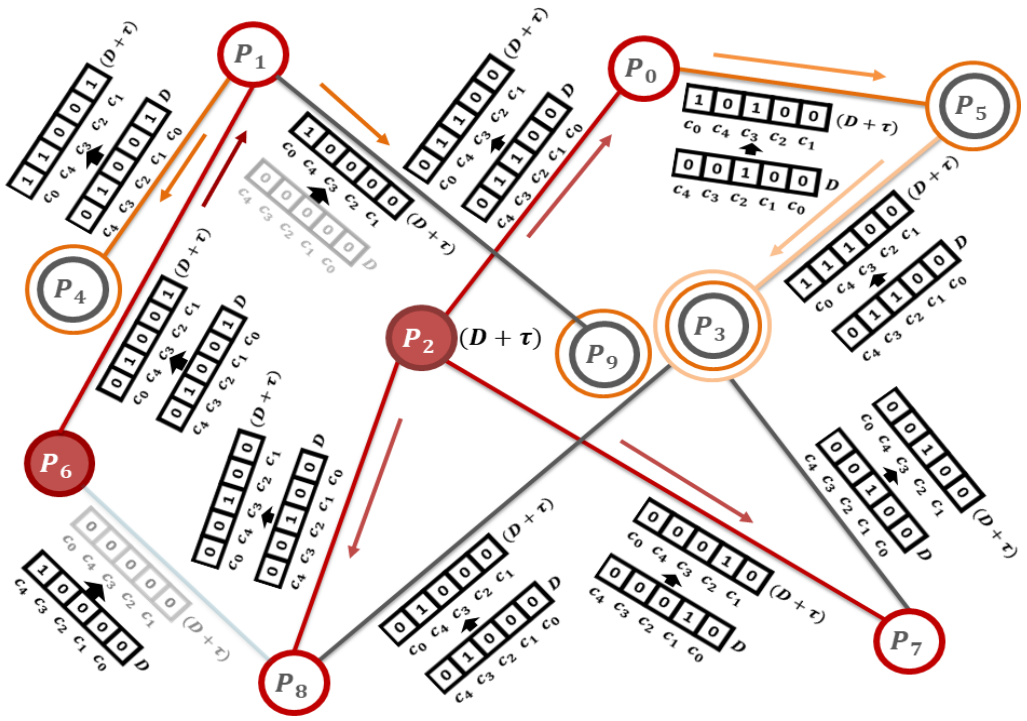


Fig. 3. Contact graph ($\mathcal{G}$) annotated with the contact vectors ($\boldsymbol{c}$) at D and $D+\tau$ time instance. Here, we consider $N = 10$ and size of $\boldsymbol{c}$ is $n = 5$. One can observe that during the D days window, there is no close contact between P_1 and P_9. However, as time progress the data streams from the devices at $D+\tau$, there is close contact between P_1 and P_9; thus, the algorithm sets one bit in $\boldsymbol{c}_{(P_1,P_9)}$. Similarly, there is an edge between P_6 and P_8 during the D days window; however, at $D+\tau$ time slot, they have no close contact; thus algorithm removes this edge and updates $\mathcal{G}$. Further, for a given infected member P_2, from $\mathcal{G}$ by analyzing associated contact vector we get first-level contact list as $\{P_0, P_7, P_8\}$, second-level as $\{P_5\}$, and third-level as $\{P_3\}$ respectively.

infections and pathways of transmissions. Once a node or set of nodes are tested to be infected within D days, then the algorithm can trace the contact of the infected person over the close contact data stored within the contact vector in $\mathcal{G}$. Therefore, a contact vector associated with an edge helps to trace the chances of a person to person infection elements transmission.

For a sufficiently large population, due to social relationships, everyone is not coming in close contact with every other [31]. That means the average number of close contact relationships q is small compared to N ($q \ll N$), and hence $\mathcal{G}$ is highly sparse. On the other hand, forming a close contact requires human mobility and coming close to each other, which is dynamic in nature. To store such sparse connectivity and the dynamic nature of human behavior, we use adjacency lists [32], [33], [34] to represent $\mathcal{G}$ under the PHA server. Here, we use optimized index-based [35] dynamic adjacency lists to maintain this fast access of ready-to-use digital form of $\mathcal{G}$ so that fetching of direct contacts for the generation of multi-level contact list becomes easy and accurate.

2.3 Contact Tracing

Using edges of graph sketch $\mathcal{G}$ for a given infected list $\mathcal{I}$, we can easily generate all the *direct contact* trace members in Γ. However, for *indirect contact* tracing we use contact trace operator σ. Here, we illustrate the contact tracing process with an example. Fig. 3 is a scenario of $\mathcal{G}$ with ten individuals $\Sigma = \{P_0, P_1, \ldots, P_9\}$ with $n = 5$ ($D = 5$ and $\tau = 1$ day). We show $\mathcal{G}$ for $5th$ and $6th$ days with the associated contact vector on the edges (Fig. 3). More details of the contact graph evolution process is portrayed in suppl. Fig. S1. Let us assume upto $5th$ day, $\mathcal{I} = \emptyset$, hence, $\Gamma = \emptyset$ (Fig. 3). On the $6th$ day P_2 and P_6 (marked as red in Fig. 3) are identified as infected ($\mathcal{I} = \{P_2, P_6\}$), hence, the PHA server initiates the contact tracing process on $\mathcal{G}$ and find the $\Gamma = \Gamma_{P_2} \cup \Gamma_{P_6}$.

2.3.1 Direct Tracing

We can observe (Fig. 3) that P_0, P_7 and P_8 are in direct close contact of P_2 in latest D days window as there are edges and corresponding contact vectors are nonzero ($P_2 \rightsquigarrow P_0$, $P_2 \rightsquigarrow P_7$ and $P_2 \rightsquigarrow P_8$). Hence, $\Gamma_{P_2} = \{P_0.1, P_7.1, P_8.1\}$ and similarly $\Gamma_{P_6} = \{P_1.1\}$

are the direct or first-level contact trace list of P_2 and P_6, respectively.

2.3.2 Indirect Tracing

To prepare the second-level (indirect) close contact list of P_2, we observe that P_3 and P_5 are possible candidates (Fig. 3). However, we can not confirm this by observing only the presence of edges and non-zero contact vectors. Now, we need to analyze the respective contact vectors. Remarkably, the listing and pruning of second and higher-level contact list can be prepared through numerical operations on the equivalent decimal integer values corresponds to the binary contact vector where c_0 as LSB and c_{n-1} as MSB of the binary number. We know that for any binary integer number, the weight of a higher significant position (2^i) is always greater than the sum of all weights at lower significant positions ($i-1$ to 0) [32]. For this reason, if the decimal value of any binary number (say $v_1 = val(\boldsymbol{c}_{(P,P')})$) is greater than equal to decimal value of another non-zero binary number (say $v_2 = val(\boldsymbol{c}_{(P',P'')})$), indicates that at least one close contact occurs earlier for the close contact vector corresponds to v_1 than all close contacts corresponds to v_2 (Lemma 1 and 2 in suppl.). We use this clue to solve the multilevel contact tracing in $\mathcal{G}$ by implementing σ.

From Fig. 3, the decimal integer values of $v_1 = val(\boldsymbol{c}_{(P_0,P_2)}) = c_4c_3c_2c_1c_0 = 11000 = 24$ and $v_2 = val(\boldsymbol{c}_{(P_0,P_5)}) = c_4c_3c_2c_1c_0 = 01001 = 9$ at $D+\tau$ time are respectively. These two bit patterns implies that at first time slot both P_0 and P_2 comes close to each other and have an close contact, but P_0 and P_5 do not have any close contact. However, on the second time slot in between (P_0, P_2) and (P_0, P_5) bits are 1, indicates they three are altogether. Hence, infection can transmit from the P_2 to P_5 via P_0 (suppl. Fig. S2). Here, $v_1 > v_2$ says at least one contact between P_2 and P_0 ($P_2 \rightsquigarrow P_0$) occurred earlier than the contact between P_0 and P_5 ($P_0 \rightsquigarrow P_5$). Hence, P_5 may get infection from P_2 via P_0 (Lemma 1 in suppl.) and thus included in the second-level contact list ($P_2 \rightsquigarrow P_0 \rightsquigarrow P_5$ or $\boldsymbol{c}_{(P_2,P_0)}\sigma\boldsymbol{c}_{(P_0,P_5)}$ evaluates to TRUE).

There are two ways P_3 can get the infection indirectly either from P_7 or from P_8. From the contact vectors $v_1 = val(\boldsymbol{c}_{(P_2,P_7)}) = 00100 = 4$ and $v_2 = val(\boldsymbol{c}_{(P_3,P_7)}) = 01000 = 8$ and thus, $v_2 > v_1$ (Suppl. Fig. S3(a)). Similarly, from $v_1 = val(\boldsymbol{c}_{(P_2,P_8)}) = 8$ and $v_2 = val(\boldsymbol{c}_{(P_3,P_8)}) = 16$, hence again $v_2 > v_1$. However, from Lemma 2 third condition fails and hence $P_2 \rightsquigarrow P_7 \not\rightsquigarrow P_3$ or $\boldsymbol{c}_{(P_2,P_7)}\sigma\boldsymbol{c}_{(P_3,P_7)}$ is FALSE, and also $P_2 \rightsquigarrow P_8 \not\rightsquigarrow P_3$ or $\boldsymbol{c}_{(P_2,P_8)}\sigma\boldsymbol{c}_{(P_3,P_8)}$ is FALSE. Hence, inclusion of P_3 into the second level contact list is not required.

Now, we test for the third level contact of P_2. During the latest D days window, P_3 comes in contact with P_5, and we already know $P_2 \rightsquigarrow P_0 \rightsquigarrow P_5$ is TRUE. Here, $v_1 = val(\boldsymbol{c}_{(P_0,P_5)}) = 01001 = 9$ and $v_2 = val(\boldsymbol{c}_{(P_3,P_5)}) = 11001 = 25$, thus $v_2 > v_1$. Therefore, following Lemma 2 both the conditions are satisfied, thus P_3 gets infection from P_2 via P_0 and P_5. Hence, by extending the transitivity relation $P_2 \rightsquigarrow P_0 \rightsquigarrow P_5 \rightsquigarrow P_3$, we can observe that P_3 will be included in the third-level contact list (Fig. 3 and Suppl. Fig. S3(b)). No further processing is possible and tracing stops with $\Gamma_{P_2} = \{P_0.1, P_7.1, P_8.1, P_5.2, P_3.3\}$, and similarly $\Gamma_{P_6} = \{P_1.1, P_4.2, P_9.2\}$. In this way, algorithm can implement σ operator and use it to prepare the indirect contact list easily and accurately from $\mathcal{G}$.

Additionally, from $\mathcal{G}$ during the contact tracing process, one can also find the infection transmission pathways very easily and here, we store inside χ as directed edges, $\chi_{P_2} = \{(P_2,P_8),(P_2,P_7),(P_2,P_0),(P_0,P_5),(P_5,P_3)\}$ and $\chi_{P_6} = \{(P_6,P_1),(P_1,P_4),(P_1,P_9)\}$, where (P_i,P_j) represents P_i transmits infection to P_j (suppl. Fig. S4). To handle large number of χ's in an efficient way, we use the disjoint set data structure and more details is in section 3.4.

3 IMPLEMENTATIONS

A particular jurisdiction has one PHA server that maintains all computations of the automated contact tracing process. We consider PHA employs Bluetooth enabled smartphones as the representatives of individuals for the automated data acquisition operations to implement the digital close contact trace system. On initialization, the PHA server creates an empty $\mathcal{G}$ along with $\mathcal{I} = \emptyset$, $\Gamma = \emptyset$ and having population $\Sigma = \{P_0, P_1, \ldots, P_{N-1}\}$. To maintain privacy (phone numbers is not shareable) during local Bluetooth based communication, the smartphone uses randomly generated virtual IDs distributed by the PHA server (suppl. section 2). Now each device individually shares the send/receive virtual IDs with a timestamp as a data stream ($\boldsymbol{\Omega}$) to the PHA server for the identification of close contact(s). As the smartphone uses the virtual ID to communicate and resolve on the PHA server-side, the privacy of the user will be maintained. In the following sections, we provide an implementation detail of $\mathcal{G}$.

3.1 Data Structure for Contact Graph Sketch

We represent $\mathcal{G}$ using adjacency lists having two components, index file ($\mathcal{G}.\Psi$) and close contact vectors file ($\mathcal{G}.\Theta$). The $\mathcal{G}.\Psi$ stores q number of index records with two fields *UserID* and *Pointer* for each user (Fig. 4). Here, q, the average degree of the $\mathcal{G}$ represents the average number of distinct persons coming in close contacts to a person during D days. Moreover, we maintain one extra index record in $\mathcal{G}.\Psi$ to move into

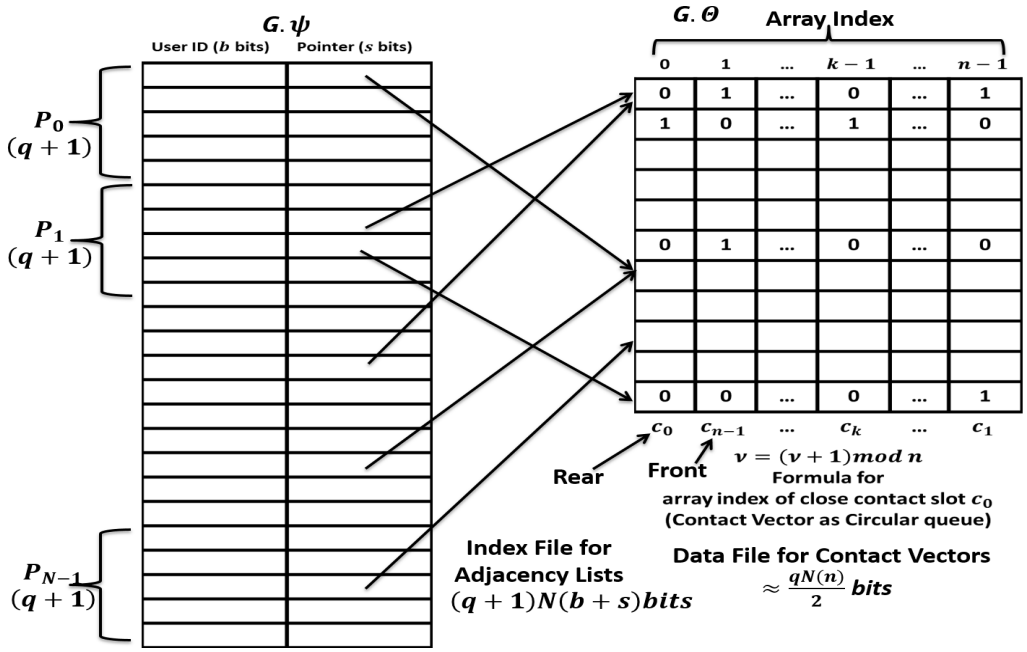


Fig. 4. Data Structure for the contact graph ($\mathcal{G}$). Here, $\mathcal{G}.\Psi$ is the index representation of adjacency lists of N persons as *(UserID, Pointer)*. The $\mathcal{G}.\Theta$ holds fixed size contact vectors $\boldsymbol{c}$ of size n. Both are in the form of array. Here, $(q+1)^{st}$ index record for each user is assigned to enter into the respective overflow area.

the overflow area when contacts exceed the average value of q for an individual.

We know for each pair of individuals P and $P^{'}$ there is an undirected edge having $\boldsymbol{c}_{(P,P^{'})}$ is the edge label. Hence, we store $\boldsymbol{c}$ only once in $\mathcal{G}.\Theta$ at A index position or address which is used as pointer field of records in $\mathcal{G}.\Psi$. For an edge $e = (P, P^{'}, \boldsymbol{c}_{(P,P^{'})})$, $P^{'}$ will appear as one record $(P^{'}, A)$ under adjacency list of P in $\mathcal{G}.\Psi$. Similarly, we keep another record (P, A) under $P^{'}$. For a particular disease parameters, D and τ are fixed, which implies, $\boldsymbol{c}_{(P,P^{'})}$ has a fixed length (n). Also, we assume, on average for an user, there is a q number of distinct close contacts during the D days period. Therefore, we can access both $\mathcal{G}.\Psi$ and $\mathcal{G}.\Theta$ as an array with constant access time. Here, algorithm uses $\mathcal{G}.\Psi[P(q+1)]$ to access the starting contact record of P. Similarly, $\mathcal{G}.\Theta[A \times n]$ to access the first bit of $\boldsymbol{c}_{(P,P^{'})}$. In addition, to access the overflow area we use $\mathcal{G}.\Psi[P(2q+1)]$ [36]. Therefore, through $\mathcal{G}$ we can watch every close contacts of the society for the latest D days, and reflect as sliding watch window with all c_0 is the close contact front of the Σ.

3.2 Embedding data stream into contact graph

The PHA server receives the contact data stream ($\boldsymbol{\Omega}$) from registered mobile devices (Fig. 5). The $\boldsymbol{\Omega}$ contains a header part and communication details with virtual IDs. The header part holds the actual sender ID as P in $\boldsymbol{\Omega}.UID$ and broadcast start time as $\boldsymbol{\Omega}.StartTime$ as t. Further, communication details contain $\boldsymbol{\Omega}.Tran$ and $\boldsymbol{\Omega}.Rec$ for transmitted and all received virtual user IDs during proximity contact (Fig. 5). A valid close contact requires τ min of continuous proximity neighbors' data. To improve the sampling accuracy we split the τ in δ time interval i.e., $\tau = \delta \times \rho$ min ($\rho > 1$ is a positive integer). Hence, if someone is present nearby with a person for a continuous ρ number of samples, then there will be a close contact. Therefore, to detect close contact during stream processing, the algorithm uses a sliding window ($\mathbf{W}$) of size ρ. For COVID-19, one can set $\delta = 3$ min, and thus, $\rho = 5$, and hence, to ensure a close contact, one person should appear 5 times inside $\mathbf{W}$.

To process stream data of mobile devices and detect close contact, we use one sliding window ($\mathbf{W}$). On the other hand, contact vector ($\boldsymbol{c}$), which always holds the latest D days binary close contact data, is another siding window. We implement the first window as a simple FIFO queue, whereas the contact vector as a circular queue (stored in a one-dimensional array), and always inserts or en-queue of data at REAR and removing or de-queue of an element from FRONT of these queue structures [32]. Hence, maintaining $\mathcal{G}$ is the interplay between two sliding windows. Here, next latest slot (c_0 at array index $\nu \leftarrow (\nu + 1) \mod n$) of $\boldsymbol{c}$ always appears at REAR and earliest slot (c_{n-1}) at the FRONT of the queue. For circular behavior of modulo-

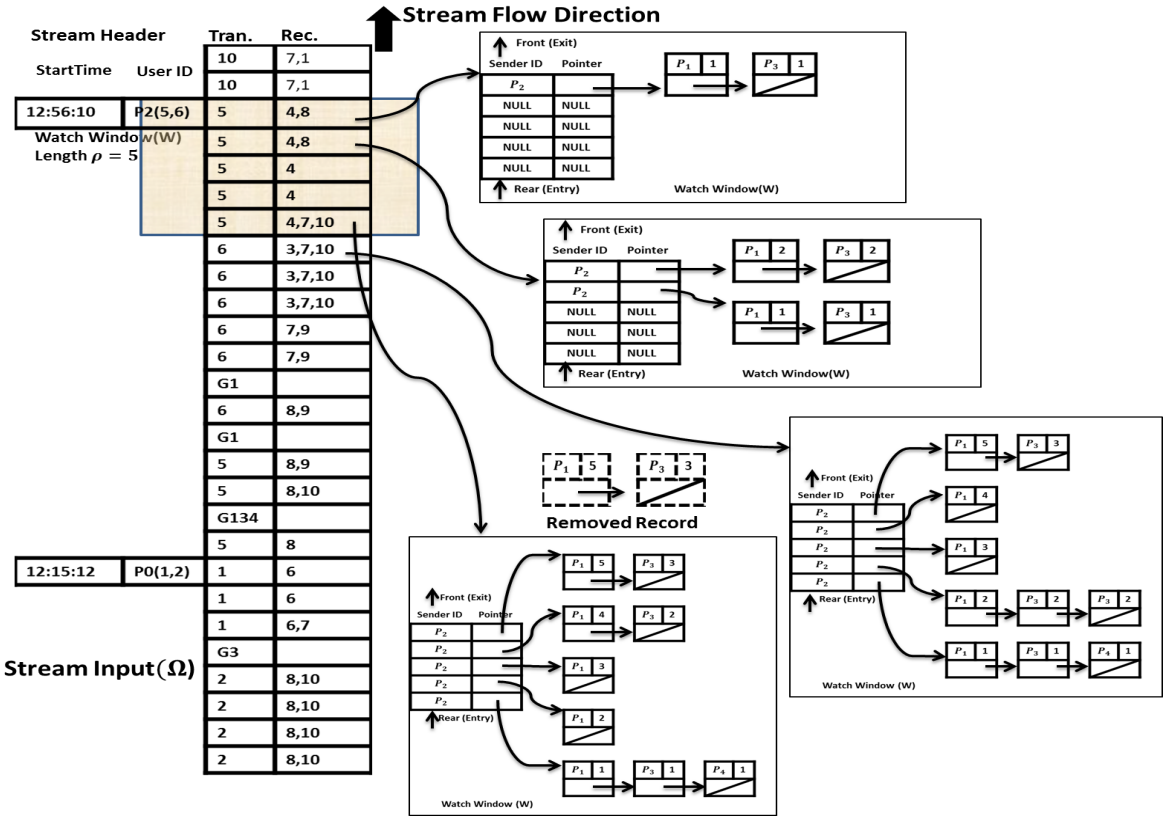


Fig. 5. Processing proximity data stream ($\mathbf{\Omega}$) and detect close contact through a watch window ($\mathbf{W}$). The PHA server assigns virtual IDs to the users P_0, P_1, ..., P_{N-1} as $\pi_{P_0} = \{1, 2\}, \pi_{P_1} = \{3, 4\}, \ldots, \pi_{P_{N-1}} = \{2N-1, 2N\}$ (suppl. section 2). Individuals' smartphones communicate through virtual IDs during the broadcast and appear in the $Tran.$ and $Rec.$ fields in $\mathbf{\Omega}$. For every user, $\mathbf{\Omega}$ begins with a start time (t) and the actual user ID of the sender. The $\mathbf{W}$ is a fixed size ($\rho = 5$) array of pointers which works as a FIFO queue where data enters at the REAR and exits from FRONT. The window and holds proximity data for the latest ρ intervals. Each entry of $\mathbf{W}$ holds the actual sender ID and the list of real receiver IDs in a linked list form. Receiver ID in $\mathbf{W}$ associates a communication count value (ϱ) to count the appearance in ρ number of intervals. During removal from FRONT of $\mathbf{W}$ if the ϱ of any user $P^{'}$ is equal to ρ then it is a close contact between P and $P^{'}$. A pointer field is NULL, means there is no proximity communication in the next interval.

arithmetic, after initialization when queue becomes full after passing D days, c_0 returns to the $\nu = 0$ array index location and c_{n-1} appears at array index 1 and so on (Fig. 4 and suppl. Fig. S5).

Now, we illustrate the functioning of sliding watch windows ($\mathbf{W}$) to detect close contact from the data stream (Ω). From Fig. 5, one can observe that Ω is the snapshot of two users' sampled data (P_2 and P_0) shared with the PHA server. After accessing the header, the server realized that P_2 start communicating with others at time $t = 12 : 56 : 10$ and uses its own virtual ID 5 and 6. Now, from virtual user IDs (4 and 8) in $\mathbf{\Omega}.Rec$ field of the current sample data associated with P_2, PHA server determines the actual user IDs (e.g., P_1 for 4, P_3 for 8) of the receiver from the ID mapping table and store temporarily in a set say $U = \{P_1, P_3\}$. Therefore, (P_2, P_1) and (P_2, P_3) are two proximity contacts in this current sample interval and stored at $\mathbf{W}[0]$ in a linked list form with associated communication count (ϱ) value set to one ($P_1.\varrho = P_3.\varrho = 1$). Similarly, server get the same situations for the next interval data, and $\mathbf{W}[1]$ stores the corresponding linked list for P_1, P_3. However, to indicate the twice appearance of users P_1, P_3 in $\mathbf{W}$, ϱ value of the earlier communication with persons in U are increased by one for record at $\mathbf{W}[0]$ ($P_1.\varrho = P_3.\varrho = 2$). Similar, processing continues until $\mathbf{W}$ is full. Now, to accommodate the next interval data at REAR, algorithm removes elements from FRONT at $\mathbf{W}[0]$. After removal, the algorithm checks the ϱ value for a user. If it is equal to ρ, then it is a close contact. Here, one can observe that for $P_1.\varrho = \rho$ (Fig. 5). Hence, P_1 was in proximity contact for latest all ρ number sample intervals leading to a close contact with P_2. Therefore, we require to install into c_0 slot of the contact vector ($\boldsymbol{c}_{(P_2,P_1)}$) in $\mathcal{G}$. However, (P_2, P_3) is not a close contact as $P_3.\varrho \neq \rho$ and not to install.

Now, to embed the detected close contact in $\mathcal{G}$,

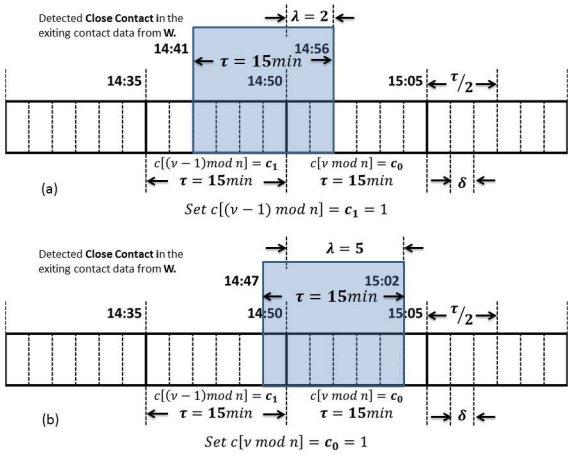


Fig. 6. Resolving the conflict between slot numbers (c_1 and c_0) of $\boldsymbol{c}$ for a detected close contact at c_0. The maximum part of the close contact duration lies (a) in c_1 slot and (b) in c_0 slot.

we determine the array index number (ν) for c_0 of $\boldsymbol{c}$ by synchronizing the start time (t) of P ($P \equiv P_2$) with the system start time (T) (Eq. 1). With the use of this time synchronization it is possible to identify every component of $\boldsymbol{c}$ and corresponding array index ν where c_0 will be located. Also, note that due to unpredictable human nature, close contact may appear at any time. That means the first sample interval of close contact may be at any of ρ number of intervals in the earlier slot, i.e., c_1 and accordingly ends at any of ρ number of sample intervals in c_0 slot (Fig. 6). In this situation, we select suitable one from c_0 and c_1 depending on the most proximity contact intervals (Fig. 6). Therefore, to make decision about c_0 and c_1, we also synchronize t of P with T for the interval number (λ) of the current array index ν (Eq. 1).

$$\nu = \left\lfloor \frac{T^{'}}{\tau} \right\rfloor \mod n, \quad \lambda = \left\lfloor \frac{T^{'}}{\delta} \right\rfloor \mod n^{'} \qquad (1)$$

where $T^{'} = (1440 \times X.Days + 60 \times X.Hrs + X.Min)$ and $X = T - t$ (date difference), here T is the system deployment time, both t and T are in format $dd/mm/yyyy : hh : mm$ and date difference $T - t$ is in format $Days/Hrs/Min$, and $n^{'} = \lfloor \frac{1440D}{\delta} \rfloor$. Further, when there is no communication for one or more δ time interval(s) between nearby Bluetooth devices, we consider the next record in $\boldsymbol{\Omega}$ is of Gx format, indicating that there is a communication gap for $x(\geq 1)$ number of δ time intervals. For Gx, we update ν and λ for starting slot (c_0) using Eq. (2) to skip x number intervals.

$$\nu = \left(\nu + \left\lfloor \frac{x}{\rho} \right\rfloor\right) \mod n, \quad \lambda = (\lambda + x) \mod \rho \quad (2)$$

Now, in Fig. 6, we show how ν and λ are used to identify correct slot in $\boldsymbol{c}$ accordingly update the detected close contact in $\mathcal{G}$. Here, $\boldsymbol{c}[\nu \mod n]$ is equivalent to c_0 slot, and $\boldsymbol{c}[(\nu - 1) \mod n]$ is the immediate earlier slot c_1.

Algorithm 1 Process($\mathcal{G}, \boldsymbol{\Omega}$)

```
while (Buffer(Ω) ≠ φ) do
  if (Ω.StartTime ≠ φ) then
    t, P ← Ω.StartTime, Ω.UID
    ν, λ, ρ, W ← Initialize(t)
  end if
  X ← GetNext(Ω.Data)
  if (X = Gx) then
    ν, λ, W ← Update(ν, λ, x)
  else
    U ← GetUsers(X.Rec, t)
    U.ϱ ← 1
    W ← UpdateCounters(W, U)
    if (Size(W) = ρ) then
      W ← Delete(W, U')
      for all (P' in U') do
        if (P'.ϱ = ρ) then
          G ← Install(G, P, P', ν, λ)
        end if
      end for
    end if
    if λ = ρ then
      ν ← (ν + 1) mod n
    end if
    λ ← (λ + 1) mod ρ
    W ← Insert(W, U)
  end if
end while
return G
```

Now, to understand the time synchronization, we divide close contact duration $\tau = 15$ min into $\rho = 6$, number of sample intervals each of length $\delta = \frac{15}{6} = 2.5$ min. Here, half of the number of sample intervals is $\lfloor \frac{\rho}{2} \rfloor = 3$. In Fig. 6 (a), we show that current close contact watch window ends before half of the number intervals of c_0 slot ($\lambda = 2 \leq \lfloor \frac{\rho}{2} \rfloor$). This indicates most of the part of current close contact exists in the immediate earlier slot, so $c_1 = 1$. Similarly, in Fig.6 (b), we show $\lambda = 5 (> \lfloor \frac{\rho}{2} \rfloor)$, that means most of part of current $\mathbf{W}$ exists in the latest slot, so $c_0 = 1$. In this way conflict for c_1 and c_0 is resolved.

Finally, we consider $Set()$ function is used to perform these changes of $\boldsymbol{c}$ in $\mathcal{G}$. The process will continue for the whole contact data stream of the different users (Algorithm 1). Algorithm 1 (suppl.) helps to install any detected close contact (P, P', ν, λ) into $\mathcal{G}$ during data stream processing. To install the close contact for P, search starts from $\mathcal{G}.\Psi[P(q+1)]$ location of the index file. If it is successful, then updating is performed in

the target slot. However, on an unsuccessful search, the algorithm creates an empty contact vector $\boldsymbol{c} = 0$ in $\mathcal{G}.\Theta$, and accordingly, we update the target slot. New contact vector means new relation between P and $P^{'}$ and hence, we also update $\mathcal{G}.\Psi$ (Algorithm 1). As time passes, the social contact dynamics are changing, and without any latest close contact, some contacts are older than incubation duration D. Hence, the PHA server removes the edge(s) along with contact vector(s) from $\mathcal{G}$.

3.3 Contact Tracing on $\mathcal{G}$

The $\mathcal{G}$ maintains the digital form of the social contact dynamics of Σ for the particular geopolitical area under a PHA for the last D days. We assume that at any time, the system has a contact trace list (Γ) for a given set of infected persons ($\mathcal{I}$). Hence, the system updates these lists using the following procedures for incoming situations. Suppose at any time, one or more individuals are detected as newly infected persons and kept in $\mathcal{I}^{'}$. After receiving $\mathcal{I}^{'}$, system starts immediate contact tracing on $\mathcal{G}$ where $\mathcal{I}^{'}$, Γ, $\mathcal{G}$ and L are passed as input parameters (Algorithm 2). Here, $L \geq 1$ means up to which level we require to trace the contacts. The algorithm returns updated Γ, which contains first, second, and other required higher levels of indirect contacts along with respective edge list $\chi^{'}$.

Finally, we update new infected list as $\mathcal{I} \leftarrow \mathcal{I} \cup \mathcal{I}^{'}$, and directed edge list to detect infection pathways as $\chi \leftarrow \chi \cup \chi^{'}$. Person appears once in contact list, Algorithm 2 automatically removes any redundancy.

The algorithm uses two queues Q_1 and Q_2 alternatively as processing and waiting of individuals to trace close contact (Algorithm 2). Initially, we set current contact level number $l = 1$ (direct or first-level contact), and all members in $\mathcal{I}^{'}$ are in the processing queue (Q_1) and hence, Q_2 is empty and working as waiting queue. Now, for all members in the Q_1 direct contact list are generated from indexed adjacency list in $\mathcal{G}.\Psi$ and stored in Γ as well as in the waiting queue (Q_2). For higher-level contact tracing we update l, swap Q_1 and Q_2, and call $TraceOperator()$ method (suppl. Algorithm 2).

In section 2.3, we explain the different such situations for filtering the second and higher-level contact tracing for which bit-patterns of $\boldsymbol{c}$ and decimal values are used to exclude or include the next member in the contact list and also pruning of further processing. The process will continue either no more individuals left in the waiting queue or the target level (L) of indirect contacts has been reached (Algorithm 2).

3.4 Disjoint Sets for Contact Trace Results

Practically the contact trace system provides suspected (Γ) and also generates the directed edge list (χ) to maintain the infection pathways (Algorithm 2). There are several general questions from the perspective of management - how many clusters of infected groups, list the members of these clusters, the order or pathways of infection spreading, i.e., infectious trees. Only Γ is not sufficient to meet these requirements. We use Disjoint Set Data structure (DSD) denoted as $\mathcal{F}$ to address the above queries [32]. Initially, for Σ, $\mathcal{F}$ maintains N number of rooted single node disjoint trees all marked with status 'Free' and $\mathcal{F}.EdgeList$ is empty. Algorithm of DSD uses the results from the contact trace algorithm to update $\mathcal{F}$. Here, the $\mathcal{F}.EdgeList$ of the DSD stores all directed edges in χ (suppl. Algorithm 3). Now, using the $union - find()$ operation of DSD, all directed edges in χ are processed to form the

Algorithm 2 TraceContacts($\mathcal{G}, \mathcal{I}^{'}, \Gamma, L$)

```
Create χ, Q1, Q2, l
for all P ∈ I' do
  A ← P(q+1)
  while G.Ψ[A].Pointer ≠ NULL do
    P' ← G.Ψ[A].UID
    if P' ∉ Γ then
      P'.Level ← l
      Γ ← Γ ∪ P'
      χ ← χ ∪ Edge(P, P')
      Q1 ← Insert(Q1, A)
    end if
    A ← A + 1
  end while
end for
l ← l + 1
while ((l ≤ L) and not (IsEmpty(Q1) and IsEmpty(Q2))) do
  while (not IsEmpty(Q1)) do
    Q1 ← Delete(Q1, A)
    P ← G.Ψ[A].UID
    A' ← P(q+1)
    while G.Ψ[A'].Pointer ≠ NULL do
      P' ← G.Ψ[A'].UID
      c1 ← G.Θ[A]
      c2 ← G.Θ[A']
      if P' ∉ Γ and TraceOperator(c1, c2) then
        P'.Level ← l
        Γ ← Γ ∪ P'
        χ ← χ ∪ Edge(P, P')
        Q2 ← Insert(Q2, A')
        A' ← A' + 1
      end if
    end while
  end while
  Q1, Q2 ⟷ Q2, Q1
end while
return Γ, χ
```

final disjoint sets. Nodes are also marked according to 'Infected' and 'Suspected'. For any individual, $find()$ returns the root of the infection tree, which means the group or cluster to which the individual belongs. Further, traversing this rooted tree provides the full cluster, size of the cluster, and the order of spreading, i.e., infectious tree. The number of such rooted trees in the $\mathcal{F}$ is the count of the disjoint sets, i.e., the number of clusters exists presently in the PHA. Each such cluster is an infection zone with separate active infections and suspected members under the isolation process. In this way, when we use the contact tracing result is stored in a DSD structure, then taking different management decisions during a pandemic becomes easy.

4 Performance Analysis

4.1 Space complexity analysis

Here, we calculate the space requirement to store the graph sketch for the D days proximity data of N number of users as adjacency list representation (Fig. 4). We know $\mathcal{G}$ has two parts $\mathcal{G}.\Psi$ for index store and $\mathcal{G}.\Theta$ for data store and space requirement is denoted as $\mathcal{S}(\mathcal{G}.\Psi)$ and $\mathcal{S}(\mathcal{G}.\Theta)$ respectively. We need $b = \lceil log_2 N \rceil$ bits to access ID of the N number of different users. Next, we assume in an average there are q number of distinct close contacts during a time period of D days or n ($n = \lceil \frac{1440D}{\tau} \rceil$) number time slots of duration τ min. For each user, we store $q+1$ number of direct index records in $\mathcal{G}.\Psi$ and for these direct records $\frac{qN}{2}$ number contact vectors each of $(n+1)$ bits (one extra bit for deletion flag) are stored in $\mathcal{G}.\Theta$. To identify each such contact vector, we require $s = \lceil log_2 \frac{qN}{2} \rceil$ bits index in the pointer field of the index record. Therefore, the space requirement for $\mathcal{G}.\Psi$ is

$$\begin{aligned}\mathcal{S}(\mathcal{G}.\Psi) &= (q+1)N(b+s) \\ &= (q+1)N(2\log N + \log q - 1) \\ &= \mathcal{O}(N \log N)\end{aligned}$$

bits. Similarly, for $\frac{qN}{2}$ number of records in $\mathcal{G}.\Theta$ is

$$\mathcal{S}(\mathcal{G}.\Theta) = \frac{qN}{2}(n+1) = \mathcal{O}(N)$$

bits. Hence, the total space requirement (in bits) is

$$\begin{aligned}\mathcal{S}(\mathcal{G}) &= \mathcal{S}(\mathcal{G}.\Psi) + \mathcal{S}(\mathcal{G}.\Theta) \\ &= N\left[(q+1)(2\log N + \log q - 1) + (n+1)\frac{q}{2}\right] \\ &= \mathcal{O}(N \log N)\end{aligned} \tag{3}$$

Study shows that for a very small percentage of cases overflow area is required [31]. Hence, the additional memory requirement will be nominal. Here, D, τ, and q are constant for a particular type of infection, and hence, we get the space complexity of $\mathcal{G}$ is $\mathcal{O}(N \log N)$.

For COVID-19 outbreak, we assume for population of $N = 10^7$, the length of infectious period $D = 14$ days, minimum time of contact $\tau = 15$ min. To estimate q, we use statistics from a recent UK based social contact survey [31]. It suggests that for COVID-19 pandemic the average number of contacts (q) over 14 days is 217. However, only 59 (27%) of contacts are meeting close contact definition [12], [31]. With this statistics, we choose $q = 64$. Hence, the estimated storage requirements for $\mathcal{G}$ using Eq. (3) is:

$$\begin{aligned}\mathcal{S}(\mathcal{G}) &= 10^7[(64+1)(2\log 10^7 + \log 64 - 1) \\ &\quad + \left(\frac{1440 \times 14}{15} + 1\right)\frac{64}{2}] \times 2^{-33}\ GB \\ &\approx 55\ GB\ as\ 1GB = 2^{33}\ bits.\end{aligned}$$

Note that for simplicity, we consider q as a constant, which implies every node has the same degree. However, in real-world situations q follows a heterogeneous degree distribution [37]. To handle this degree heterogeneity in the real-world implementations, we maintain an overflow area in $\mathcal{G}$.

4.2 Time complexity

The system has three parts for the operation - (a) detecting and then storing of digital close contacts during stream processing, (b) tracing of multi-level contacts for a set of infected individuals, and (c) storing tracing results in the disjoint set data structure to answer different standard management and control operations.

To detect a close contact in $\mathbf{\Omega}$ and installation into $\mathcal{G}$, requires maximum q number array index manipulations. We assume q is constant and independent of N, thus average number of computation required for the processing of $\mathbf{\Omega}$ is constant and hence, time complexity is $\mathcal{O}(1)$. The $\mathcal{G}$ is a ready to use form for contact tracing. Computation complexity for the preparation of Γ has two parts - computation counts for direct list preparation denoted as $(T_{direct}(q, L, n, N))$ and for indirect list as $(T_{indirect}(q, L, n, N))$. Now, we evaluate $T_{direct}(q, L, n, N)$ for given $\mathcal{I}$ as follows. For any infected person P in $\mathcal{I}$, we access at most q number of consecutive pointer field in $\mathcal{G}.\Psi$ array. We know that one can reach to the beginning of the adjacency list of P using $\mathcal{G}.\Psi[P(q+1)]$ (section 3.1). Therefore, total pointer comparison count takes

$$T_{direct}(q, L, n, N) = q \times |\mathcal{I}| = \mathcal{O}(q|\mathcal{I}|) \tag{4}$$

However, to prepare the second level contact list, we perform n bits contact vector comparison to execute σ for each members in the direct contact list of $q \times |\mathcal{I}|$ individuals (Algorithm 2) is $q \times (q \times |\mathcal{I}|)$, and for

third-level it is $q \times (q^2 \times |\mathcal{I}|)$ and so on. Hence, the total computation complexity for indirect levels is

$$\begin{aligned} T_{indirect}(q, L, n, N) &= n[q \times (q \times |\mathcal{I}|) + q \times (q^2 \times |\mathcal{I}|) \\ &\quad + \ldots + q \times (q^{L-1} \times |\mathcal{I}|)] \\ &= q^2 \times \frac{(q^{L-1} - 1)}{(q-1)} \times (|\mathcal{I}| \times n) \\ &= \mathcal{O}(q^L |\mathcal{I}|) \end{aligned}$$

Now, for both direct and indirect contact list tracing computation takes

$$T(q, L, n, N) = \mathcal{O}(q^L |\mathcal{I}|)$$

Finally, for disjoint set representation having $|\Gamma|$ of contact trace members with $|\chi|$ number edges takes $\mathcal{O}(|\chi|\alpha(|\Gamma|))$ where $\alpha()$ is the *Inverse Ackermann()* function, $\alpha() \leq 5$ [32]. From the above analysis, we can show that for COVID-19 contact trace parameters, to prepare the contact list for a given $\mathcal{I}$, it takes $\mathcal{O}(|\mathcal{I}|)$ when q and L are constant.

5 Conclusion

In this article, we design a dynamic graph streaming algorithm with sophisticated data structures for a digital contact tracing system to mitigate the spreading of a contagious outbreak under the control of the Public Health Authority of a country. After receiving the data stream from the mobile devices, the algorithm uses a sliding window model to convert continuous proximity-based device data into the discrete close contact slots and convert it into a fixed-length bit pattern and stored in the contact vector. Finally, in the server, all close contact vectors use to form an efficient dynamic contact graph sketch. Once the server maintains the close contact graph sketch, our algorithm prepares the direct and indirect (multilevel) contact list of the infected persons and stores it in disjoint sets. We use the index file structure to store the large contact graph in an array. Here, we use two sliding windows to process the stream data of mobile devices and detection of close contacts and another sliding window used to maintain the close contact vector over D days period. The first one is implemented as a FIFO queue, and the second one is implemented as a FIFO circular queue. Our framework is relevant to general contact-transmitted diseases like COVID-19 and can trace digital contact for other relevant infectious diseases by changing the parameters of our algorithm (incubation period and proximity duration of contacts). Heart of our algorithm is the contact trace operator, which uses numerical computation over the binary number stored inside the contact vector to decide the multilevel contact trace list. Our analysis unveils that for COVID-19 outbreak close contact parameters, the storage space requires maintaining the contact graph of 10^7 individuals having 14 days close contact data in PHA server takes 55 Gigabytes of memory and prepares the contact list for $\mathcal{I}$ takes $\mathcal{O}(|\mathcal{I}|)$.

The binary representation of close contact is an integral part of our algorithm. Importantly, interactions between a pair of the individual are annotated as a binary circular vector to elucidate the communication in a different time and capture a complete picture of the social interactions. Therefore, dynamic contact graph sketch reflects the population dynamics of the jurisdiction and can be used for further study related to epidemic dynamics to predict the trajectory of the spread accurately [19]. Here, we develop the algorithm relevant to the proximity data of Bluetooth enabled mobile devices. However, we can easily extend the algorithm for Global Positioning Systems (GPS) based sensor data with some modification, and further research [20]. Although our goal is to provide a space-efficient and easily accessible digital contact tracing algorithm under the control of PHA and prepare the direct as well as indirect contact list, however, considering the virtual ID and binary contact vector, the algorithm implicitly enforces the privacy of users. For more details of the privacy concern of the digital contact trace, we refer to the current articles [18], [38], [39]. On the other hand, the sliding window model is space-efficient and can have a further application from the applied and theoretical perspectives to analyze the streaming data [40]. We consider the mobility of users under one PHA. Our model can be extended to design hierarchical and distributed forms to make this more manageable and concurrently operable.

The main objective of this Information Technology (IT) based system is to make solutions feasible to computation, and that can control the further transmission of diseases. However, as in practical situations, we should also follow other pre-existing processes like social distancing, partial lockdown, preventive measures like washing hands, and disinfection to control infections.

Acknowledgment

Gautam Mahapatra acknowledges Post-graduate Division of Asutosh College, University of Calcutta for financial support and computational resources. Priodyuti Pradhan acknowledges Bar-Ilan University for providing Kolman-Soref postdoctoral fellowship.

References

[1] R. Hinch et al., Effective configurations of a digital contact tracing App: A report to NHSX, 2020.
[2] Singh, Rajesh and Adhikari, Ronojoy, Age-structured impact of social distancing on the COVID-19 epidemic in India, arXiv preprint arXiv:2003.12055, 2020.
[3] Karin, Omer et al., Adaptive cyclic exit strategies from lockdown to suppress COVID-19 and allow economic activity, medRxiv, Cold Spring Harbor Laboratory Press, 2020.

[4] Meidan, Dror and Cohen, Reuven and Haber, Simcha and Barzel, Baruch, An alternating lock-down strategy for sustainable mitigation of COVID-19, Accepted Nature Communications, arXiv preprint arXiv:2004.01453, 2020.
[5] Mark Zastrow, Coronavirus contact-tracing apps: can they slow the spread of COVID-19?, Nature, 2020.
[6] Kelly Servick, COVID-19 contact tracing apps are coming to a phone near you. How will we know whether they work?, Science, 2020.
[7] Hellewell, Joel et. al, Feasibility of controlling COVID-19 outbreaks by isolation of cases and contacts, The Lancet Global Health, Elsevier, 2020.
[8] Megan Scudellari, The Pandemic's Future,Nature News Feature, 2020.
[9] World Health Organization and others, Coronavirus disease 2019 (COVID-19): situation report, 107, World Health Organization, 2020.
[10] De Carli, A and Franco, M and Gassmann, A and Killer, C and Rodrigues, B and Scheid, E and Schoenbaechler, D and Stiller, B, WeTrace–A Privacy-preserving Mobile COVID-19 Tracing Approach and Application, arXiv preprint arXiv:2004.08812, 2020.
[11] Ferretti, Luca and Wymant, Chris and Kendall, Michelle and Zhao, Lele and Nurtay, Anel and Abeler-Dörner, Lucie and Parker, Michael and Bonsall, David and Fraser, Christophe, Quantifying SARS-CoV-2 transmission suggests epidemic control with digital contact tracing, Science 368 (6491), 2020.
[12] Keeling, Matt J and Hollingsworth, T Deirdre and Read, Jonathan M, The Efficacy of Contact Tracing for the Containment of the 2019 Novel Coronavirus (COVID-19), medRxiv, Cold Spring Harbor Laboratory Press, 2020.
[13] T. TraceTogether, "How does TraceTogether work?", https://tracetogether:zendesk:com/hc/en-sg/articles/360043543473-How-does-TraceTogether-work-,2020, accessed: 2020-03-23.
[14] , Covid Watch, urlhttps://www.covid-watch.org/, accessed: 2020-05-11, 2020.
[15] , Sydney Von Arx, Daniel Blank, Slowing the Spread of Infectious Diseases Using Crowdsourced Data, Covid Watch, 2020.
[16] Rivest, R et. al, The PACT protocol specification, 2020.
[17] Privacy-Preserving Contact Tracing, 2020. https://www.apple.com/covid19/contacttracing,accessed:2020-05-11
[18] Government of India, Aarogya Setu Mobile App, 2020. https://www.mygov.in/aarogya-setu-app/,Accessed:09-05-2020
[19] Oliver, Nuria et. al, Mobile phone data for informing public health actions across the COVID-19 pandemic life cycle, American Association for the Advancement of Science, 2020.
[20] Hernández-Orallo, Enrique and Manzoni, Pietro and Calafate, Carlos T and Cano, Juan-Carlos, Evaluating how smartphone contact tracing technology can reduce the spread of infectious diseases: the case of COVID-19, IEEE Access, 2020.
[21] Amit, Moran and Kimhi, Heli and Bader, Tarif and Chen, Jacob and Glassberg, Elon and Benov, Avi, Mass-surveillance technologies to fight coronavirus spread: the case of Israel, Nature Medicine, 2020.
[22] Maxmen, Amy, Can tracking people through phone-call data improve lives?, Nature, 569(7758), 2019.
[23] Ben Lovejay, Turing algorithms may improve accuracy of Apple/Google contact tracing API, 2020. https://9to5mac.com/2020/06/29/turing-algorithms/,accessed:2020-06-29
[24] Allen, Danielle, Securing Justice, Health, and Democracy against the COVID-19 Threat, 2020.
[25] Christina Potter, 'Zero COVID-19 Deaths in Vietnam', https://www.outbreakobservatory.org/outbreakthursday-1/7/9/2020/zero-covid-19-deaths-in-vietnam,accessed:2020-07-19
[26] Moneycontrol News, WHO warning on COVID-19: 'Not even close to being over. Worst is yet to come', 2020. https://www.moneycontrol.com/news/trends/health-trends/coronavirus-pandemic-worst-is-yet-to-come-who-wars-5480611.html,accessed:2020-
[27] Bar-On, Yinon M and Flamholz, Avi and Phillips, Rob and Milo, Ron, Science Forum: SARS-CoV-2 (COVID-19) by the numbers, eLife 9, e57309 2020.
[28] Ebola and Contact Tracing, https://www.cdc.gov/cdctv/diseaseandconditions/outbreaks/ebola-contact-tra
[29] Influenza (Avian and other zoonotic) https://www.who.int/news-room/fact-sheets/detail/influenza-(avian-and-oth
[30] Statista, Smartphone users 2020, Data Access – 03.12.2020. https://www.statista.com/statistics/330695/number-of-smartphone-users-worl
[31] Danon, Leon and Read, Jonathan M and House, Thomas A and Vernon, Matthew C and Keeling, Matt J, Social encounter networks: characterizing Great Britain, Proceedings of the Royal Society B: Biological Sciences, 280(1765), 2013.
[32] Cormen, Thomas H and Leiserson, Charles E and Rivest, Ronald L and Stein, Clifford, Introduction to algorithms, 2009, MIT press.
[33] West, Douglas Brent, Introduction to graph theory, 1996, Prentice hall Upper Saddle River, NJ.
[34] Deo, Narsingh, Graph theory with applications to engineering and computer science, 2017, Courier Dover Publications.
[35] Silberschatz, Abraham and Korth, Henry F and Sudarshan, Shashank, Database system concepts, McGraw-Hill New York, 1997.
[36] Garcia-Molina, Hector and Ullman, Jeffrey D and Widom, Jennifer, Database system implementation, Prentice Hall Upper Saddle River, NJ, 2000.
[37] A-L Barabási, *Network Science*, Cambridge University Press, (2016).
[38] Bengio, Yoshua et. al, The need for privacy with public digital contact tracing during the COVID-19 pandemic, The Lancet Digital Health, Elsevier, 2020.
[39] Mello, Michelle M and Wang, C Jason, Ethics and governance for digital disease surveillance, Science 368(6494), 951-954, 2020.
[40] McGregor, Andrew, Graph stream algorithms: a survey, ACM SIGMOD Record 43(1), 9-20, ACM New York, NY, USA, 2014.

arXiv:2007.05637v3 [cs.DS] 4 Dec 2020

Supplementary Information: Dynamic Graph Streaming Algorithm for Digital Contact Tracing

Gautam Mahapatra[1,2], Priodyuti Pradhan[3], Ranjan Chattaraj[2], and Soumya Banerjee[4]

1. Computer Science, Asutosh College, University of Calcutta, Kolkata, West Bengal, India
2. Computer Science and Engineering, Birla Institute of Technology, Mesra, Off-Campus Deoghar, Jharkhand, India
3. Complex Network Dynamics, Department of Mathematics, Bar-Ilan University, Ramat-Gan, Israel
4. Inria EVA, Paris, France & Director Innovation Smart City EU.

Disclaimer: Our digital contact trace management software is in the developing phase. We have implemented the server-side coding (module 2) as well as the prototype of the mobile app is also developed. We are preparing a separate manuscript for the details of module 1. Please visit the GitHub link to download the app and codes `https://github.com/OTwo-DCT/OTwoAndroid`.

1 Close contact graph evolution

Here, we illustrate the dynamic evolution of the close contact graph $\mathcal{G}$ by the sequence of diagrams in Fig. S1 for Day-1 to Day-6 with five days contact vector. In Day-1 there is a close contact between P_6 and P_8, so queue REAR at leftmost position or at zero index of the array and this is c_0. For Day-2, Day-1 is earliest and Day-2 is the latest, so the Day-1 close contact is now c_1, and for Day-2 it is c_0. Here, array index advances for one. This process continues up to Day-5. For Day-6, there is no space to store close contact data for this day. However, we implement this for the latest five days, so the Day-1 contact information exiting from the front, i.e., zero position of the array, and here latest close contact c_0 is stored at this zero-index location and all $c_i^{'}$s are shifted one place right, so c_4 now appears at array index one and so on. Also, on Day-6, we find close contact between P_6 and P_8 is more than five days old and hence automatically disconnected from the graph. It is also confirmed that P_2 and P_6 are detected as infected, and contact tracing on this close contact data from the vectors shows the possible flow of the direct, first level, and second level indirect infection transmission pathways. Note that P_9 first time come in close contact on Day-6, and may get infection of P_6 via P_1.

2 Virtual ID distribution by PHA server

A particular jurisdiction has one PHA server that maintains all processing of the automated contact tracing process. We consider PHA employs Bluetooth enabled smartphones as the representatives of individuals for the automated data acquisition to implement the digital close contact trace system. Every smartphone user must have a unique phone number used as the identity of the phone calls and all other services. To maintain privacy during local Bluetooth communications, it is not possible to know the assigned phone number of a nearby person comes into social contacts [1]. Hence, our system uses virtual IDs for Bluetooth-based data acquisitions. After deployment, in a regular interval, the PHA server randomly generates a set of virtual IDs for whole populations $\Sigma = \{P_0, P_1, \ldots, P_{N-1}\}$. For this purpose, PHA server sub-divided the non-negative natural numbers ($\mathbb{N}$) into N numbers of non-overlapping sets each of size $r(\geq 1)$, i.e., $\pi = \{\pi_1, \pi_2, \ldots, \pi_N\}$, where $\pi_i = \{k_1, k_2, \ldots, k_r\}$, $\pi_i \cap \pi_j = \emptyset$, $|\pi_i| = r$, $k_i \in \mathbb{N}$. The PHA server assigns this pi_i to the different members in Σ. Consider P and $P^{'}$ are two distinct Bluetooth enabled smartphones. Let $\pi_P \equiv \pi_i$ and $\pi_{P'} \equiv \pi_j$ assigned virtual IDs sets for P and $P^{'}$ respectively. Next, P and $P^{'}$ randomly choose $k_i \in \pi_P$ and $k_j \in \pi_{P'}$ and used as virtual IDs. As both P and $P^{'}$ are having multiple assigned IDs, in a specific period, they can use separate k_i and k_j as their virtual IDs. Consider P and $P^{'}$ are two distinct Bluetooth

enabled smartphones. Now, when both P and P' (or others) come in social contact with a minimum (d) distance confirmed by the Bluetooth signals, respective devices broadcast messages using their virtual IDs in δ time intervals [2]. During this communication, P receives messages from P' with a used virtual ID and vice-versa. Now each device individually stores and share the send/receive virtual IDs with a timestamp as a data stream ($\mathbf{\Omega}$) to the PHA server to identify the close contact(s). As smartphone uses the virtual id to communicate, and this will be resolve in the PHA server-side; hence it maintains the users' privacy.

2.1 Sampling of contacts by the smartphones

To improve the accuracy of the temporal proximity data acquisitions captured by the Bluetooth enabled devices, the contact tracing system further subdivides each τ minutes time slots into ρ numbers of sampling time intervals each of δ minutes ($\tau = \delta \times \rho$, $\rho > 1$ is a nonzero positive integer). Therefore, for D days $n^{'} = \lceil \frac{1440D}{\delta} \rceil$ number of data samples are to be processed. Note that close contact and data samples are different, which means the ρ number of consecutive samples implies one close contact. Now, when both P and P' (or others) come in social contact with a minimum distance (d) confirmed by the Bluetooth signals, respective devices broadcast messages using their virtual IDs in δ time intervals [2]. During this communication, P receives messages from P' with a used virtual ID and vice-versa. These transmitted and received messages are locally stored in the device memory and the send/receive timestamp. Finally, devices pre-process the proximity data locally and send as data stream represented as $\mathbf{\Omega}$ to the PHA server to identify the close contact(s).

Algorithm 1 Install($\mathcal{G}, P, P^{'}, \nu, \lambda$)

[Check for existing contact vector between P and $P^{'}$]
$A_1 \leftarrow Search(\mathcal{G}.\Psi, P, P^{'})$
if $(A_1 \neq NULL)$ **then**
  $A \leftarrow \mathcal{G}.\Psi[A_1].Pointer$
else
  [Get an empty contact vector for $\mathcal{G}.\Theta$]
  $A, \mathcal{G}.\Theta \leftarrow GetContactVector(\mathcal{G}.\Theta)$
  [Get an empty record for the edge $(P, P^{'})$ under adjacency list of P]
  $B_1, \mathcal{G}.\Psi \leftarrow GetIndexRec(\mathcal{G}.\Psi, P)$
  [Insert record for the edge $(P, P^{'})$]
  $\mathcal{G}.\Psi[B_1].UID \leftarrow P^{'}$
  $\mathcal{G}.\Psi[B_1].Pointer \leftarrow A$
  [Get an empty record for the edge $(P^{'}, P)$ under adjacency list of $P^{'}$]
  $B_2, \mathcal{G}.\Psi \leftarrow GetIndexRec(\mathcal{G}.\Psi, P^{'})$
  [Insert record for the edge $(P^{'}, P)$]
  $\mathcal{G}.\Psi[B_2].UID \leftarrow P$
  $\mathcal{G}.\Psi[B_2].Pointer \leftarrow A$
end if
$\mathcal{G}.\Theta \leftarrow Set(\mathcal{G}.\Theta[A], \nu, \lambda)$
return $\mathcal{G}$

3 Contact trace operator ($\boldsymbol{\sigma}$)

Let us consider $\boldsymbol{c}_{(P,P')}$ and $\boldsymbol{c}_{(P',P'')}$ are two stored contact vectors among three individuals $P, P^{'}$ and $P^{''}$ (Fig. 2(c)). Now, if P comes outs as laboratory-confirmed infected person then $P \rightsquigarrow P^{'}$ returns TRUE, hence $P^{'}$ appears as direct contact trace, but $P^{''}$ appears as an indirect contact trace only when we can justify

that there is possibility of transmission of infection elements from P to $P^{''}$ via $P^{'}$. To make a decision, we need both contact vectors $\boldsymbol{c}_{(P,P^{'})}$ and $\boldsymbol{c}_{(P^{'},P^{''})}$. Here, σ act as a binary operator on $\boldsymbol{c}_{(P,P^{'})}$ and $\boldsymbol{c}_{(P^{'},P^{''})}$ i.e., $\boldsymbol{c}_{(P,P^{'})}\sigma\boldsymbol{c}_{(P,P^{''})}$. If $P^{''}$ has a close contact with $P^{'}$ during or after the close contact between $P^{'}$ and P within D days then σ returns TRUE, otherwise FALSE. This operator is equivalent to asking whether $P \rightsquigarrow P^{'} \rightsquigarrow P^{''}$ is TRUE or not.

Lemma 1. Let $\boldsymbol{c}_1 = \boldsymbol{c}_{(P,P^{'})} = c_{n-1}\dots c_0$ and $\boldsymbol{c}_2 = \boldsymbol{c}_{(P^{'},P^{''})} = c^{'}_{n-1}\dots c^{'}_0$ are two nonzero binary contact vectors. Suppose P is identified as an infection carrier, and $val(\boldsymbol{c}_1) \geq val(\boldsymbol{c}_2)$, then there is a possibility of infection transmission from P to $P^{''}$ via $P^{'}$ where $val(\cdot)$ returns the decimal value of the binary contact vector.

Proof. We know that for a binary number weight of the m^{th} bit position (2^m) is always greater than sum of all weights ($\sum_{i=0}^{m-1} 2^i = 2^m - 1$) at lower significant positions (0 to $m-1$). So for the given contact vectors we can write

$$c_m 2^m > \sum_{i=0}^{m-1} c_i 2^i,\ c_m = 1,\ \forall i, c_i \in \{0,1\},\ 1 \leq m \leq n-1 \tag{S1}$$

This is also true for $\boldsymbol{c}_2$. Now, given

$$val(\boldsymbol{c}_1) \geq val(\boldsymbol{c}_2) \tag{S2}$$

we will show the possibility of infection transmit from P to $P^{''}$ via $P^{'}$. If $val(\boldsymbol{c}_1) = val(\boldsymbol{c}_2) \neq 0$, then $c_i = c^{'}_i,\ \ \forall i = 0,\dots n-1$, and $\exists i$ such that $c_i = c^{'}_i = 1$. This implies in the last D days period while P is in close contact with $P^{'}$, then $P^{'}$ is also in close contact with $P^{''}$. Therefore, there is a possibility of infection transmission from P to $P^{''}$ via $P^{'}$ when $val(\boldsymbol{c}_1) = val(\boldsymbol{c}_2)$. Now, for $val(\boldsymbol{c}_1) > val(\boldsymbol{c}_2)$ (Eq. S2,), we have two following cases:

Case I: Earliest or most significant m ($0 \leq m < n$) number of slots or bits are one. Then considering Eq. S1 and Eq. S2, we get the following formats for the contact vectors:

$$\begin{aligned}\boldsymbol{c}_1 &= 1\dots 1 c_{n-m-2}\dots c_0\\ \boldsymbol{c}_2 &= 1\dots 0 c^{'}_{n-m-2}\dots c^{'}_0\end{aligned}$$

Now, if $m = 0$ then, after a close contact between P and $P^{'}$ at the earliest slot i.e. at $n-1$, there is at least one close contact between $P^{'}$ and $P^{''}$ at any slot in between 0^{th} to $(n-2)^{th}$ slot (as $val(\boldsymbol{c}_2) \neq 0$). Therefore infection transmission from P to $P^{''}$ via $P^{'}$ is possible. If $m > 0$ then, while P is in close contact of $P^{'}$, then $P^{'}$ is also in close contact of $P^{''}$ for one or more time slots, so said infection transmission is always possible.

Case II: Earliest or most significant m ($0 \leq m < n$) number of slots or bits are zero. Then considering Eq. S1 and Eq. S2 we get the following formats for the contact vectors:

$$\begin{aligned}\boldsymbol{c}_1 &= 0\dots 1 c_{n-m-2}\dots c_0\\ \boldsymbol{c}_2 &= 0\dots 0 c^{'}_{n-m-2}\dots c^{'}_0\end{aligned} \tag{S3}$$

As $\boldsymbol{c}_2$ is nonzero, so there is at least one close contact between $P^{'}$ and $P^{''}$ after the earliest close contact between P and $P^{'}$. Therefore infection transmission from P to $P^{''}$ via $P^{'}$ is always possible, and hence, the statement of the lemma is true.

Example 1 – Application of Lemma 1. Let us consider P_1, P_2 and P_3 three individuals and there are edges between (P_1, P_2) and (P_2, P_3). Respective nonzero contact vectors are $\boldsymbol{c}_1 = c_7\dots c_0$ and $\boldsymbol{c}_2 = c^{'}_7\dots c^{'}_0$ and all are 8 bits. Now using Lemma 1, we like to observe the situations for possible transmission of infection from P_1 to P_3 using P_2 as via or indirect path. Assume that P_1 is detected as an infected person.

For ($\boldsymbol{c}_1 = \boldsymbol{c}_2$): Bit-wise both are equal, and at least for one place corresponding bit values is 1. Let us consider a situation for this as follows:

$$\begin{aligned} \boldsymbol{c}_1 &= \boldsymbol{c}_{(P_1,P_2)} = 10010010 \\ \boldsymbol{c}_2 &= \boldsymbol{c}_{(P_2,P_3)} = 10010010 \end{aligned} \tag{S4}$$

For these bit patterns we find that during time slots c_7, c_4 and c_1 while P_1 is in close contact with P_2, then P_2 is also in close contact of P_3, so infection transmission from P_1 to P_3 via P_2 is possible.

For ($\boldsymbol{c}_1 > \boldsymbol{c}_2$):
Case I. Earliest or most significant few bits are equal and *all are ones*. Let us consider a situation for this as follows:

$$\begin{aligned} \boldsymbol{c}_1 &= \boldsymbol{c}_{(P_1,P_2)} = 1110000 \\ \boldsymbol{c}_2 &= \boldsymbol{c}_{(P_2,P_3)} = 1100010 \end{aligned} \tag{S5}$$

For these bit patterns we observe that during time slots c_7 and c_6 while P_1 is in close contact with P_2, then P_2 is also in close contact of P_3. Again, after an earlier close contact between P_1 and P_2, at time slot c_5 there is one latest close contact between P_2 and P_3 at time slot $c_1^{'}$. Therefore, through these close contacts infection may transmit from P_1 to P_3 via P_2.

Case II. Earliest or most significant few bits are equal and *all are zeros*. Let us consider a situation for this as follows:

$$\begin{aligned} \boldsymbol{c}_1 &= \boldsymbol{c}_{(P_1,P_2)} = 0010001 \\ \boldsymbol{c}_2 &= \boldsymbol{c}_{(P_2,P_3)} = 0000110 \end{aligned} \tag{S6}$$

For these bit patterns we observe that after earliest close contact between P_1 and P_2 at time slot c_5, there is two later close contacts between P_2 and P_3 at consecutive time slots $c_2^{'}$ and $c_1^{'}$. Therefore, through these close contacts infection may transmit from P_1 to P_3 via P_2.
By this example, we show that when $\boldsymbol{c}_1 \geq \boldsymbol{c}_2$ then infection transmission is possible through the indirect or via a path, and hence the Lemma 1.

Lemma 2. Let $\boldsymbol{c}_1 = \boldsymbol{c}_{(P,P')} = c_{n-1}c_{n-2}\dots c_0$ and $\boldsymbol{c}_2 = \boldsymbol{c}_{(P',P'')} = c_{n-1}^{'}c_{n-2}^{'}\dots c_0^{'}$ are two nonzero contact vectors. Suppose P is identified as infection carrier. Then, there is no infection transmission between P and $P^{''}$ via $P^{'}$ i.e., $\boldsymbol{c}_1\sigma\boldsymbol{c}_2$ returns FALSE, only when all three conditions (a) $val(\boldsymbol{c}_2) > val(\boldsymbol{c}_1)$, (b) earliest or most significant m $(0 \leq m < n)$ number of bits are equal and all are zeros, and (c) there is no earlier close contact between P and $P^{'}$ before the latest close contact between $P^{'}$ and $P^{''}$ are satisfied where $val(\cdot)$ returns the decimal value of the binary contact vector.

Proof. For nonzero contact vectors, with $val(\boldsymbol{c}_1) < val(\boldsymbol{c}_2)$ (condition (a)), if earliest or most significant $m \geq 1$ bits are equal and all ones, then during earliest m time slots, while P and $P^{'}$ are in close contact, then $P^{'}$ and $P^{''}$ are also in close contact, and hence infection transmission from P to $P^{''}$ via $P^{'}$ is possible and we stop here. For conditions (a) and (b), if earliest or most significant m $(0 \leq m < n)$ number of bits are equal and all zero, then we may discard these bits. After discarding we get contact vectors of the form

$$\begin{aligned} \boldsymbol{c}_1 &= 0c_{n-m-2}\dots c_0 \\ \boldsymbol{c}_2 &= 1c_{n-m-2}^{'}\dots c_0^{'} \end{aligned} \tag{S7}$$

in view of S1. Now, let at latest j^{th} time slot there is a close contact between $P^{'}$ and $P^{''}$. That means $c_j^{'} = 1$, and $c_{j-1}^{'}\dots c_0^{'} = 0\dots 0$. Also, there is an earliest i^{th} time slot where there is a close contact between P and $P^{'}$. That means $c_{n-m-2}\dots c_{i+1} = 0\dots 0$ and $c_i = 1$. For $\forall i, j \in \{0, 1, \dots n-m-2\}$. Now, if $i \geq j$, then the condition (c) fails, and after a close contact between P and $P^{'}$ there is a close contact between $P^{'}$ and

$P^{''}$, so infection transmission from P to $P^{''}$ via $P^{'}$ is possible. But, if $i < j$, then there is no close contact between $P^{'}$ and $P^{''}$ after any close contact between P and $P^{'}$. Therefore infection transmission from P to $P^{'}$ is not possible, and hence the Lemma statement is true.

Example 2 – Application of Lemma 2. Let us consider P_1, P_2 and P_3 three individuals, and there are edges between (P_1, P_2) and (P_2, P_3). Respective nonzero contact vectors are $\boldsymbol{c}_1 = c_7 \dots c_0$, and $\boldsymbol{c}_2 = c_7^{'} \dots c_0^{'}$, and all are 8 bits. Now using Lemma 2, we like to observe the situations for possible transmission of infection from P_1 to P_3 using P_2 as via or indirect path. Assume that P_1 is detected as an infected person.

Conditions (a) $val(\boldsymbol{c}_2) > val(\boldsymbol{c}_1)$ **(b) earlier or most significant bits are equal and *all are zeros*.** Let us consider one such situation:

$$\begin{aligned} \boldsymbol{c}_1 &= \boldsymbol{c}_{(P_1,P_2)} = 00000011 \\ \boldsymbol{c}_2 &= \boldsymbol{c}_{(P_2,P_3)} = 00100100 \end{aligned} \tag{S8}$$

For these bit patterns we observe that the latest close contact between P_2 and P_3 occurs at the time slot $c_2^{'}$, and the earliest close contact between P_1 and P_2 occurs at c_1 time slot, which is not before latest close contact of P_2 and P_3 and hence condition (c) is satisfied for Lemma 2. Therefore, all three conditions are satisfied, and transmission of infection from P_1 to P_2 via P_2 is not possible. Again, let us consider another such situation:

$$\begin{aligned} \boldsymbol{c}_1 &= \boldsymbol{c}_{(P_1,P_2)} = 0001011 \\ \boldsymbol{c}_2 &= \boldsymbol{c}_{(P_2,P_3)} = 00100100 \end{aligned} \tag{S9}$$

Here, conditions (a) and (b) for Lemma 2 are true, whereas (c) fails, that means we get an earliest close contact between P_1 and P_2 at time slot c_3 which is before the latest close contact between P_2 and P_3 at the time slot $c_2^{'}$, and hence infection transmission is possible from P_1 to P_3 via P_2.

Conditions (a) $val(\boldsymbol{c}_2) > val(\boldsymbol{c}_1)$ **(b) earlier or most significant bits are equal and *all are ones*.** then while P_1 is in close contact with P_2, then P_2 is also in close contact of P_3. Therefore, through these close contacts infection may transmit from P_1 to P_3 via P_2. Therefore, through Lemma 2 it is possible to know at which situation infection transmission via indirect path is not possible.

3.1 Implementation of σ

The pseudo-code (Algorithm 2) is the simple implementation of σ operator. Here $\boldsymbol{c}_1$ and $\boldsymbol{c}_2$ are two input contact vectors passed as input parameters. Now, using these two contact vectors, our contact trace operator decides whether $P^{''}$ is getting an infection from P via $P^{'}$ or not, and accordingly, we can include $P^{''}$ into the contact trace list (Γ). This implementation of the σ operator uses the equivalent decimal integer values of the binary contact vectors and then Lemma 1 and 2 for the processing. Here, v_1 and v_2 are respectively the decimal equivalent of $\boldsymbol{c}_1$ and $\boldsymbol{c}_2$. After conversion here we try to validate through the condition of Lemma 1, i.e. $v_1 \leq v_2$. If fails, then we apply the conditions for the Lemma 2. Here, earliest close contact for $\boldsymbol{c_1}$ (i.e. left most 1 in $\boldsymbol{c_1}$) and latest close contact for $\boldsymbol{c}_2$ (i.e. right most 1 in $\boldsymbol{c_2}$) both are determined by the sequential traversal of the contact vectors. Finally, it returns either TRUE or FALSE. Note that if number is negative then all most significant bits are ones, otherwise zeros. This can be used for the checking whether most significant n^{th} bit is 1 or not (here n is the length of the contact vector).

4 Security and Privacy Issues

For our system, the graph sketch ($\mathcal{G}$) is holding individuals' contact data in a binary encoded form (contact vector - $\boldsymbol{c}$). This encoded contact data is a location independent data model of the whole social contact structure (Σ) under the custody of the concerned PHA. Using suitable private key cryptography, we can easily protect the whole graph data from corruption. Locally captured discrete contact data is also not storing

Algorithm 2 TraceOperator($\boldsymbol{c}_1, \boldsymbol{c}_2$)

[Convert binary contact vectors $\boldsymbol{c}_1$ and $\boldsymbol{c}_2$ into equivalent decimal integers]
$v_1 \leftarrow val(\boldsymbol{c}_1)$
$v_2 \leftarrow val(\boldsymbol{c}_2)$
[Process the trivial indirect transmission]
if $v_1 \geq v_2$ **then**
  return TRUE
end if
[Process the non-trivial indirect transmission]
if $\boldsymbol{c}_1[n-1] = 1$ **and** $\boldsymbol{c}_1[n-1] = \boldsymbol{c}_2[n-1]$ **then**
  return TRUE
end if
[Sequentially process the earliest and latest close contacts from $\boldsymbol{c}_1$ and $\boldsymbol{c}_2$]
$i \leftarrow Earliest\ \ Close\ \ Contact\ \ of\ \ \boldsymbol{c}_1$
$j \leftarrow Latest\ \ Close\ \ Contact\ \ of\ \ \boldsymbol{c}_2$
if $i > j$ **then**
  return FALSE
else
  return TRUE
end if

any location data and the actual time of contact. Our system only uses samples proximity-based presence of two low-power Bluetooth enable mobile phones and captures as locally stored discrete contacts. It uses randomly selected virtual-ID from a set of virtual-IDs assigned by the PHA server and updated regularly for privacy reasons. With these brief descriptive views, we can justify the system's reliability after maintaining security and privacy measures.

Algorithm 3 BuildDisjointSet($\mathcal{F}, \chi, \mathcal{I}, \Gamma$)

[Process each directed edges in χ]
while ($\chi \neq \phi$) **do**
  [Get next edge from input edge list]
  $\xi \leftarrow RemoveNext(\chi)$
  [Store the edge in the edge list of $\mathcal{F}$]
  $A \leftarrow Insert(\mathcal{F}.EdgeList, \xi)$
  [Use $Find()$ operation to locate the root nodes for both the nodes of the edge]
  $i \leftarrow Find(\mathcal{F}, \xi.P)$
  $j \leftarrow Find(\mathcal{F}, \xi.P^{'})$
  [Check for cycle formation]
  if $i \neq j$ **then**
    [When there is no cycle, then use $Union()$ operation for merging the trees for the nodes of the edge]
    $\mathcal{F} \leftarrow Union(\mathcal{F}, i, j, A)$
  end if
end while
return $\mathcal{F}$

References

[1] T. TraceTogether, "How does TraceTogether work?", `https://tracetogether:zendesk:com/hc/en-sg/articles/360043543473-Ho` accessed: 2020-03-23.
[2] Zhong, Xin, Bluetooth Low Energy Application in home automation, 2019.

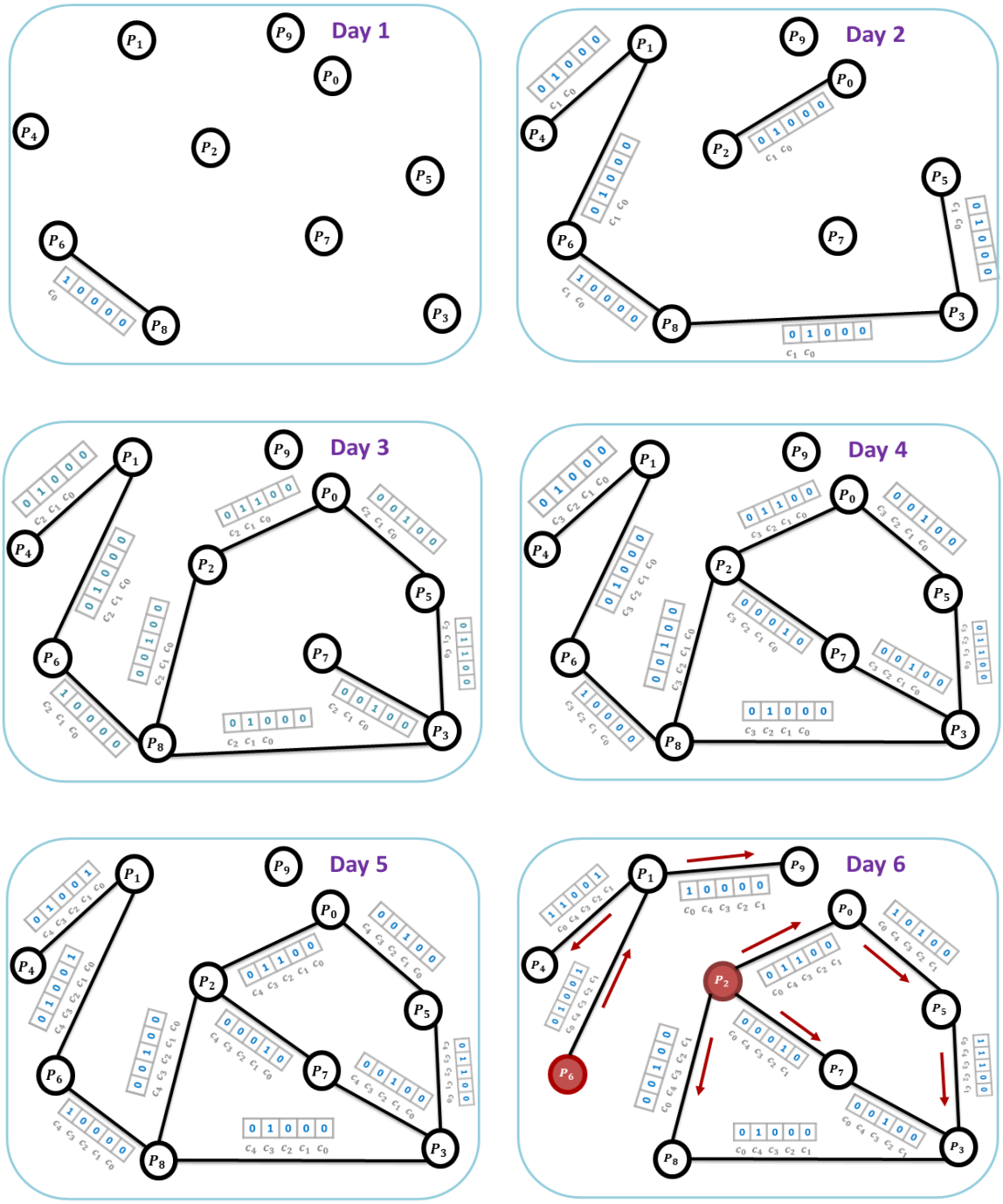


Fig. S1. Dynamic evolution of close contact graph for six days.

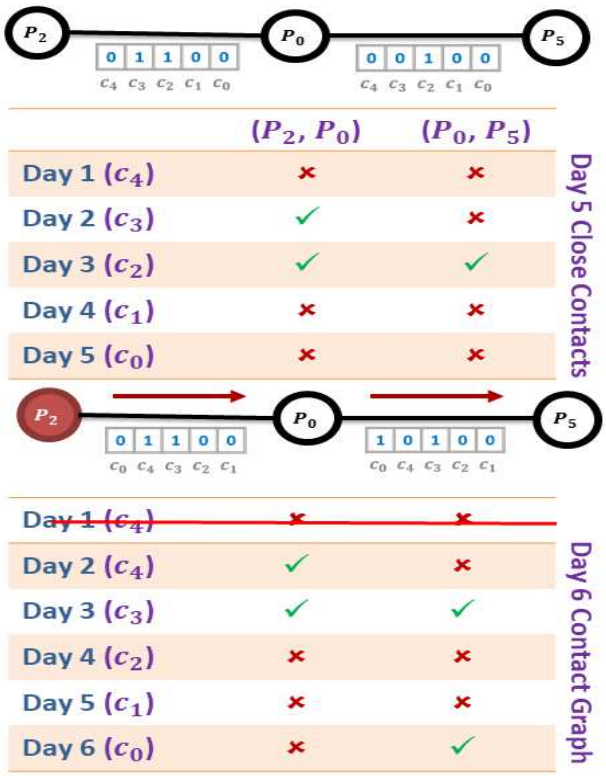


Fig. S2. Illustration of contact tracing!

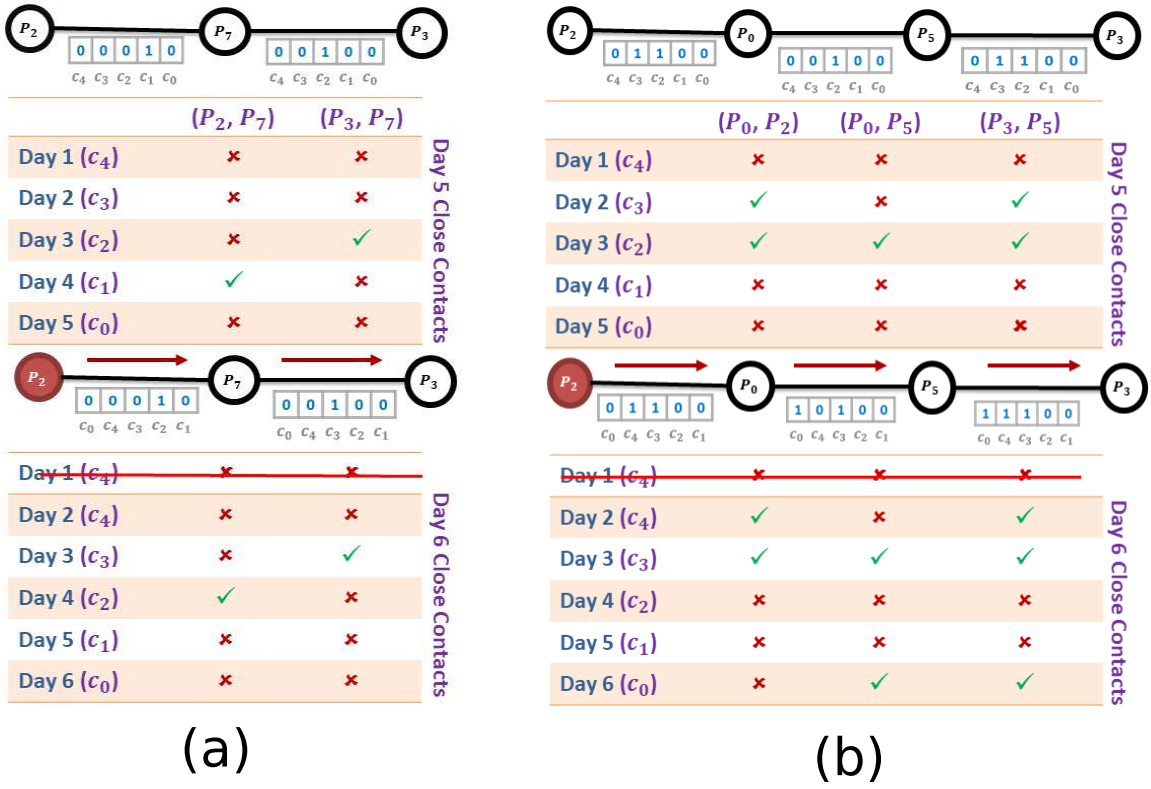


Fig. S3. Illustration of contact tracing!

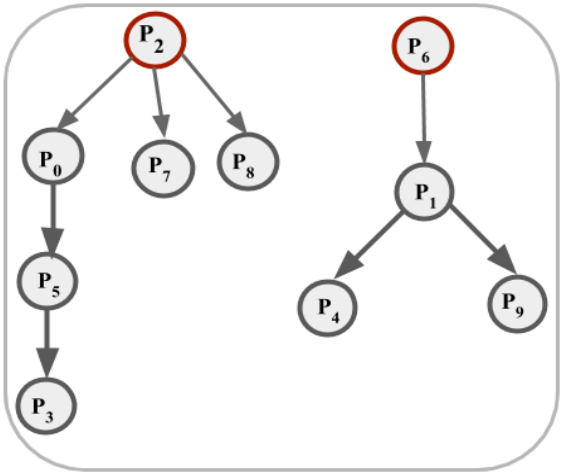


Fig. S4. Infection pathways. $\chi_{P_2} = \{(P_2, P_8), (P_2, P_7), (P_2, P_0), (P_0, P_5), (P_5, P_3)\}$ where (P_i, P_j) represents P_i transmits infection to P_j, holds the infection transmission pathways. Similarly, $\chi_{P_6} = \{(P_6, P_1), (P_1, P_4), (P_1, P_9)\}$.

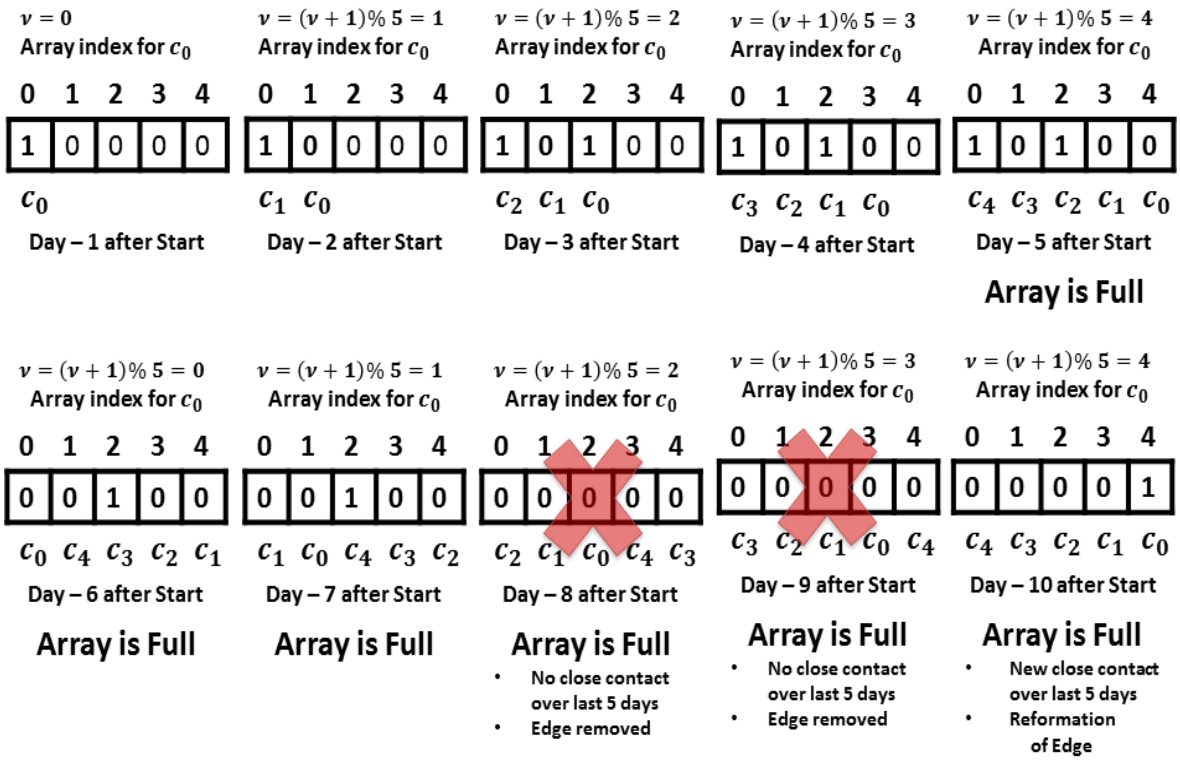


Fig. S5. Illustration of the array-based circular queue implementation using modular-arithmetic for sliding window of the contact vector $\boldsymbol{c}_{(P,P')}$ in $\mathcal{G}$. For simplicity, we consider $D = 5$ days, $\tau = 1$ day, so size of the contact vector is $n = 5$. After D days $\boldsymbol{c}_{(P,P')}$ attends the full length. Here, $\boldsymbol{c} = 0$ means there is no close contact during the latest D days, so the possibility of infection transmission is nullified, and hence respective edge will be removed. However, they may come in close contact again. A new contact vector will be formed after synchronization with system deployment time.